THE LIFT COEFFICIENT OF FLAT PLANING SURFACES

Donald David Farshing, Jr.

THE LIFT COEFFICIENT OF FLAT PLANING SURFACES

A Thesis Submitted in Partial Fulfillment
of the Requirements for the Degree of
Master of Science

STEVENS INSTITUTE OF TECHNOLOGY

Submitted by Donald David Farshing, Jr.

TABLE OF CONTENTS

ABSTRACT

A theoretical and experimental investigation to determine the lift coefficient of a flat plate planing surface covering a broad range of trim angles and aspect ratios is presented.

The analysis is divided into two principal parts: first considered is the modification of the two-dimensional potential flow solution for the effect of a finite span neglecting gravity; then, second, the effects of gravity on the finite span planing surface are discussed with the importance of Froude Number emphasized.

The analysis made on the effect of a finite span neglecting gravity is accompanied by an experimental investigation in which angles of trim up to 30 degrees and wetted length-beam ratios up to about seven are explored.

The analytical approach leads to the prediction of reasonable values for the lift coefficient, but to get better agreement with experimental data, an empirical correction factor is introduced.

The investigation, conducted at the Experimental Towing Tank, Stevens Institute of Technology, Hoboken, N. J., is the thesis submitted by the author in partial fulfillment of the requirements for the degree of Master of Science.

NOTATION

τ	Geometric angle of trim
λ	Wetted length-beam ratio $(\frac{}{b})$
C_V	Speed coefficient (Froude Number) $V/\sqrt{gb}$
g	Acceleration of gravity
b	Beam of planing surface or span of airfoil
V	Velocity of the free stream
C_L	Lift coefficient, $\frac{L}{\frac{1}{2}\rho V^2 b\ell}$
L	Lift force
ρ	Fluid density
ℓ	Wetted length of planing surface or chord of airfoil
AR	Aspect ratio, $\frac{1}{\lambda}$ or $\frac{b^2}{S}$
S	Projected wing area, $\iint_S dydx$
F	Normal force
α_e	Ambient flow angle of attack
α_i	Induced angle of attack
δ	Spray thickness
$v_{i\infty}$	Induced downwash velocity infinitely far aft
$\dot{m}$	Virtual mass rate of flow, $V\rho Vol.$
KE	Kinetic energy
ΔKE	Change in kinetic energy
r	Wetted length measured from trailing edge to stagnation line on planing surface
A	$0.4\tau^2$
B	$\frac{\pi}{2\lambda} + 4 \sin\tau$

$\frac{\Delta \ell}{b}$	Empirical wave rise factor
$\frac{\ell_1}{b}$	Wetted length-beam ratio neglecting wave rise
η_1, η_2	Empirical correction factor

Notation Used in the Section on the Effect of Gravity

ϕ	Velocity potential
U	Free stream velocity
ξ, η	Coordinates of point (x,y) on a planing surface
(x,y,z)	Coordinates of a point in space
κ	Wave number $\frac{g}{U^2}$
μ	Coefficient introduced by Maruo to obtain desired value of certain integrals
$P_s(\xi,\eta)$	Pressure at any point on planing surface
θ	Wave direction angle
k	General wave number
w	Downwash as used by Maruo
ψ	A function of Froude Number
B	Buoyancy force (Archimedian Force)

Notation in Appendix I

α	Geometric angle of attack
α_e	Ambient flow angle of attack
α_i	Induced angle of attack
w	Complex potential
ϕ	Velocity potential
ψ	Stream function
z	Complex variable, $z = x + iy$

T	Kinetic energy
S	Surface
v	Transverse flow velocity

Notation in Appendix II

R	Force
R_x	Drag force
Q	Volume flow in spray jet, $Q = V\delta$
α	Angle of trim
R_δ	Spray resistance
D	Total lift force, dynamic plus Archimedian
R_{tp}	Frictional Force
R_B	Wave resistance
ν	A function of Froude Number, $= \frac{1}{2\,Fr^2}$
Fr^2	Froude Number squared, $\frac{V^2}{g\ell}$
M	Moment
C_Z	Lift coefficient (C_L)
ℓ_d	Center of pressure location from trailing edge
$\bar{P}$, $\bar{S}$, $\bar{R}$	Vector forces
h	Depth of fluid from free surface

THE LIFT COEFFICIENT OF FLAT PLANING SURFACES

INTRODUCTION

Hydrodynamic phenomena arising from planing on the surface of water have aroused considerable interest in seaplane hull, float, and hydroski enthusiasts. In the past the need for immediate design data for floats or hydroskis has led, based on many specific experimental investigations, to the development of numerous empirical formulae to describe the flat plate lift coefficient as it varies with other parameters such as angle of trim, τ, wetted length-beam ratio, λ, and Froude Number, $V/\sqrt{gb}$. While these empirical formulae agree very well with experimental results within the range of values for which they were developed, the validity of such formulae outside the range of data for which they were developed becomes unreliable or at least questionable.

The objective of this work is to develop on a rational basis, insofar as possible, a formula for the lift coefficient of a flat plate which planes on the surface of water. At present, a rationally derived formula developed by H. Wagner, Ref. 1, covers the infinite span case, neglecting gravity, while the more recent work of L. I. Sedov, Ref. 2, and H. Maruo, Ref. 3, covers the infinite span including the effect of fluid gravity which involves wavemaking as well as hydrostatic

effects. Methods of correction for the effect of a finite span neglecting gravity have been developed by such writers as B. V. Korvin-Kroukovsky, Byrne Perry, W. Bollay, W. G. A. Perring and L. Johnston, W. Sottorf, L. Landweber, F. W. S. Locke, and C. L. Shuford, Jr., Ref. 4-12, but the entire process, including the effects of trim, aspect ratio, and Froude Number, has not been integrated except in a preliminary form.

This work involves an investigation of the methods and applicability of derivations previously made by the investigators of flat-plate planing. The problem of deriving a formula on a rational basis is treated in two distinct parts. First, the aspect ratio, trim angle effect, neglecting gravity, is considered; then, second, the effects of gravity including wavemaking are discussed.

To extend the range of experimental data for comparison with results developed analytically, an experimental investigation was made which is described herein.

The investigation has been conducted by Lt. D. D. Farshing, Jr., U.S.N., a Naval Postgraduate School student at the Experimental Towing Tank, Stevens Institute of Technology, Hoboken, New Jersey. Acknowledgement is made to Professor B. V. Korvin-Kroukovsky of the Experimental Towing Tank for his helpful guidance and interest in this work. Gratitude is also expressed to the members of the Towing Tank staff who have willingly given their assistance and advice throughout the course of this investigation.

MODIFICATION OF THE TWO-DIMENSIONAL PLANING SOLUTION FOR THE EFFECT OF A FINITE SPAN IN A WEIGHTLESS FLUID

Historical Background

There have been several attempts to find closed form solutions to the finite span planing surface problem, but difficulty arises in that formulation of the problem to satisfy the boundary conditions introduces a non-linear integral equation. Solution of the integral equation is feasible only after many simplifying assumptions have been made.

To circumvent the difficulty arising from the integral equation, another approach is offered. An ideal weightless fluid is assumed to exist. Based on the method of potential flow, a two-dimensional solution is found, then modified for the effect of a finite span by a technique similar to that used for correcting the two-dimensional airfoil to finite span.

A brief but comprehensive review of the significant work in planing up to 1949 has been presented by William Siler, Ref. 13. Charles L. Shuford, Jr., Ref. 12, has given a recapitulation of the results of many investigators who sought to find a simple formula for the three-dimensional lift coefficient of the planing flat plate. After his review of the attempts of other investigators to find simple formulas, Shuford proposes another method for predicting the lift coefficient. Shuford observes that experimental data indicates a non-linear relationship between the angle of trim and the planing lift coefficient

for the planing surface of finite span. To account for the non-linearity, he approaches the problem with an analogy to the low aspect ratio airfoil. Appendix II shows further justification for this approach. To arrive at a final total lift formula, Shuford combines three components; the first, a linear term given as one-half the value of the flat plate airfoil lift coefficient based on the lifting line theory; the second, a non-linear, cross flow term which is shown to be proportional to $\sin^2\tau$; and the third, a suction component of lift existing at the leading edge of the airfoil but not present in the planing surface flow.

Shuford's total lift formula becomes

$$C_L = \frac{\pi/2 \; AR\,\tau}{1+AR} (1 - \sin^2\tau) + \sin^2\tau \cos\tau$$

values of which agree well with experimental data. The analysis by Shuford, while in good agreement with the available experimental data, is not completely theoretical since the planing problem was not solved, but, instead, the airfoil problem manipulated.

In many of the papers concerned with modification of the two-dimensional solution for the effect of finite span, methods similar to those used for correcting the infinite span airfoil have been used with varying degrees of success. The technique of adopting similar methods seems to be a logical approach since the flow is assumed ideal (without friction) and weightless.

Another successful approach is one made by Byrne Perry, Ref. 6. Perry has applied the low aspect ratio airfoil analysis of F. Weinig, Ref. 14, to the low aspect ratio planing surface. Weinig solved the

airfoil problem without recourse to the two-dimensional solution. He applied the momentum theorem to a control surface around the airfoil with virtual mass and induced angle of attack as independent variables. The virtual mass used by Weinig is that associated with the lifting line plus a wedge of fluid found by the projection of wetted length normal to the flow:

$$\ell \sin \tau. \quad \text{(See Fig. 1)}$$

Appendix I presents more in detail the concept of virtual mass and the work of Weinig insofar as it is understood. In order to justify the choice of virtual mass made by Weinig, the applicable work of M. M. Munk, Ref. 15, is also discussed. The formulation of the low aspect ratio airfoil problem and its solution by William Bollay, Ref. 16, is considered appropriate for discussion in Appendix I, and it is compared with the solution obtained by Weinig.

The principal objection to the planing surface analysis by analogy with the low aspect ratio airfoil of Weinig is that the method for obtaining the induced angle of attack is not clear.

The Two-Dimensional Solution

H. Wagner, whose applicable work on planing is found in Ref. 1, obtained a two-dimensional solution to the planing problem. As previously stated, an inviscid, weightless fluid is assumed to exist. Coordinate axes are fixed in the planing surface which has infinite span and infinite forward length. Fluid is allowed to flow toward the plate parallel to the x axis shown in Fig. 2. The mass of fluid

of thickness δ contained between the free surface and the stagnation streamline as shown on Fig. 2 is deflected forward along the plate. The fluid below the stagnation streamline continues aft and finally becomes part of the wake. With the aid of the mathematics of complex variables using conformal transformations, Wagner finds the normal force per unit width of the infinite span to be:

$$F = \frac{\rho}{2}\ell V^2 \frac{2\pi \sin\tau}{1 + \cos\tau - (1 - \cos\tau)\ln\frac{1-\cos\tau}{2\cos\tau} + \pi\sin\tau}$$

The projection of this hydrodynamic force perpendicular to the direction of flow gives the lift force per unit span. Then:

$$L = \frac{\rho}{2}\ell V^2 \frac{2\pi \sin\tau\cos\tau}{1 + \cos\tau - (1 - \cos\tau)\ln\frac{1-\cos\tau}{2\cos\tau} + \pi\sin\tau}$$

or

$$\frac{C_L}{\text{unitspan}} = \frac{2\pi \sin\tau\cos\tau}{1 + \cos\tau - (1 - \cos\tau)\ln\frac{1-\cos\tau}{2\cos\tau} + \pi\sin\tau} \qquad (1)$$

For the infinite span case, $\tau = \alpha_t$ and $\alpha_i = 0$.

Application of the Momentum Theorem - Method I

Let us now take the infinite span solution of Wagner and modify it for the effect of finite span.

To begin we must put a control surface around the finite span planing surface so that the momentum theorem can be applied. For the control surface let us choose a solid shape of infinite spanwise width. One face is infinitely far ahead of the planing surface; one infinitely far aft; one at infinite depth below; and the remaining face at the free surface, a,b,c,d,e,f of Fig. 2.

There is no momentum flux through the side and lower faces of the control surface, so we can focus our attention of the fore and aft faces and that part of the free surface face which cuts through the forward spray.

Infinitely far ahead of the planing body, the flow is uniform and parallel to the undisturbed free surface, while infinitely far aft, a constant downwash, $v_{i\infty}$, is achieved. The downwash concept in airfoil theory is well established and is permissible in an ideal fluid without gravity. In the real fluid, frictional forces as well as gravity wave formation invalidate the discussion of a downwash infinitely far behind; however, what happens physically behind the airfoil or planing surface is not important as long as the mathematical formulation of the phenomena occurring at the body is mechanically compatible with the assumptions made about the fluid.

With the established concept of a downwash infinitely far aft of the planing body, and no downwash infinitely far ahead, it can be seen that there will be a change of momentum in the negative Z direction. Momentum flux resulting from the forward spray occurs at the control surface cutting through the spray, c d on Fig. 2. The time rate of total momentum change gives a force in the Z direction, and this force on the fluid is applied by the planing body.

Let us now consider the rectangular flat surface of finite beam planing at velocity V. If we fix axes in the planing body, the flow picture is that shown in Fig. 2. The flow about the plate can be resolved into two components, viz., a component along the plate and one

transverse to the plate. It is the transverse component of the flow which for the moment becomes important. The transverse component of flow gives rise to a virtual mass described by Wagner to be the mass of a semi-circular cylinder of fluid. The virtual mass is not a physically existing mass of fluid but it does take on physical significance. Appendix I describes how the virtual mass concept comes into existence, but for the present, suffice it to say that Wagner has found the virtual mass associated with the transverse component of flow about the planing body to be one-half that associated with the lifting line. M. M. Munk, Ref. 15, shows how one finds the virtual mass of the lifting line by association with the potential flow solution of transverse flow about a line immersed in the fluid. Munk's work is further discussed in Appendix I. Extension of the transverse flow about a line to the case of the planing plate is almost trivial, and the results lead to the mass of a semi-circular cylinder of diameter equal to the span.

The force of the plate on the fluid results from the time rate of change of the product of the virtual mass and an appropriate velocity. Similar to Weinig's low aspect ratio airfoil theory, the virtual mass associated with large values of wetted length-beam ratio planing surfaces becomes the mass of the semi-circular cylinder plus the mass of fluid found by $\ell \sin\tau$ where ℓ is wetted length and τ the angle of trim (see Fig. 1).

Justification for using the virtual mass similar to that used by Weinig, and justification for describing the virtual mass as Weinig

has done, may be found in Appendix I.

From the above analysis, we find the time rate of change of momentum from the inlet face to outlet face of the control surface to be:

$$F_Z = \dot{m}\, v_{i\infty} - \text{vertical component of spray momentum} \tag{2}$$

where

$$\dot{m} = \left(\frac{\pi b^2}{8} + \ell b \sin\tau\right)\rho V$$

One should note that the F_Z in equation (2) is the force of the planing body directed vertically down (in the negative Z direction). To find the actual lift on the planing body, F_Z, it is necessary to eliminate the spray force. Let us define $\dot{m}_s$ as the mass rate of flow in the spray. Then

$$\dot{m}_s = \rho V b \delta$$

where δ is the spray thickness (see Fig. 2).

The lift equation by application of the momentum theorem then becomes:

$$L = \left(\frac{\pi b^2}{8} + \ell b \sin\tau\right) \rho V v_{i\infty} - \rho V b \delta\, V \sin\tau \tag{3}$$

If equation (3) is divided by 2V we have

$$\frac{L}{2V} = \rho V \left(\frac{\pi b^2}{8} + \ell b \sin\tau\right) \frac{v_{i\infty}}{2V} - \frac{\rho V^2 b \delta \sin\tau}{2V} \tag{4}$$

Transposing the spray term of equation (4) to the left side, then dividing by the coefficient of $v_{i\infty}/2V$ we have:

$$\frac{L - \rho V^2 b \delta \sin\tau}{2\rho V^2 \left(\frac{\pi b^2}{8} + \ell b \sin\tau\right)} = \frac{v_{i\infty}}{2V} \tag{5}$$

Defining the length beam ratio as:

$$\frac{\ell}{b} = \lambda$$

and the lift coefficient, C_L as:

$$C_L = \frac{L}{\frac{1}{2}\rho V^2 b\ell}$$

equation (5) becomes:

$$\frac{C_L + 2\,\delta/\ell\,\sin\tau}{(\frac{\pi}{2\lambda} + 4\sin\tau)} = \frac{v_{i\infty}}{2V} \qquad (6)$$

It now becomes necessary to discuss $v_{i\infty}/2V$. At a great distance ahead of the planing body, we found the flow parallel to the free surface or, in other words, the downwash velocity zero ($v_{i-\infty} = 0$). At the center of lift of the planing body, we assume the downwash to be some fractional part of the final downwash velocity infinitely far aft of the body. For the moment, let us call the downwash velocity at the body $k\,v_{i\infty}$, where k is a fraction. From the momentum equation (neglecting spray), the force on the body is:

$$F = -\dot{m}\,v_{i\infty}$$

and the work per unit time done by the body on the fluid

$$\text{Work} = F\,k\,v_{i\infty}$$

The kinetic energy per unit time associated with the downwash infinitely far aft is:

$$KE = \frac{\dot{m}}{2}\,v_{i\infty}^{\;2}$$

while at infinite distance ahead it is zero. The change in kinetic energy isequivalent to the work done so that:

$$\Delta KE = \frac{\dot{m}}{2}\,v_{i\infty}^{\;2} = \dot{m}\,k\,v_{i\infty}^{\;2}.$$

From this analysis, it is evident that k must equal 1/2 so that at the center of lift of the planing body the downwash is one-half its value at an infinite distance aft. Now it should be clear that $v_{i\infty}/2V$ is the slope of the flow at the center of lift of the planing surface, and the angle whose tangent is $v_{i\infty}/2V$ is called the induced angle of attack or induced angle of trim. Symbolically:

$$\tan \alpha_i = \frac{v_{i\infty}}{2V}$$

Equation (6) now becomes:

$$\frac{C_L + 2\frac{\delta}{\ell}\sin\tau}{\left(\frac{\pi}{2\lambda} + 4\sin\tau\right)} = \tan\alpha_i \tag{7}$$

An inspection of Fig. 1 shows the relationships between the induced angle, α_i, the geometric trim angle, τ, and the ambient flow angle, α_e.

$$\tau = \alpha_e + \alpha_i \tag{8}$$

Let us now return attention to equation (1) which is the two-dimensional solution of the planing flat plate as developed by H. Wagner. The angle of trim τ in the two-dimensional case is equivalent to the ambient flow angle, α_e, since the induced angle is zero when gravity is not considered. Replacing τ by α_e in equation (1) and assuming α_e sufficiently small, the following approximations can be made:

$$\cos\alpha_e \approx 1$$

$\dfrac{1-\cos\alpha_e}{2\cos\alpha_e}$ is fractional and its natural logarithm is negative.

$-(1-\cos\alpha_e)\ln\dfrac{1-\cos\alpha_e}{2\cos\alpha_e}$ is positive but very small.

The denominator of (1) then becomes:

$$1 + \cos\alpha \cong 2$$

and the lift coefficient becomes:

$$C_L = \frac{2\pi \sin\alpha_e}{2 + \pi \sin\alpha_e} \qquad (9)$$

Now it becomes necessary to perform some algebraic manipulation upon equation (9).

$$\frac{C_L}{2} = \frac{2\pi \sin\alpha_e}{4 + 2\pi \sin\alpha_e}$$

$$\frac{C_L - 2}{2} = \frac{\cancel{2\pi \sin\alpha_e} - 4 - \cancel{2\pi \sin\alpha_e}}{4 + 2\pi \sin\alpha_e}$$

$$C_L - 2 = \frac{-4}{2 + \pi \sin\alpha_e}$$

$$\pi \sin\alpha_e = \frac{-4}{C_L - 2} - 2$$

$$\sin\alpha_e = \frac{-(\cancel{4} + 2\,C_L - \cancel{4})}{\pi(C_L - 2)}$$

$$\sin\alpha_e = \frac{2\,C_L}{\pi(2 - C_L)}$$

$$\alpha_e = \arcsin \frac{2\,C_L}{\pi(2 - C_L)}$$

Expanding the arc sin in series:

$$\alpha_e = \frac{2C_L}{\pi(2 - C_L)} + \frac{8C_L^3}{6\pi^3(2 - C_L)^3} + \ldots.$$

For values of $C_L \leqslant .85$, the cubic term is less than 3% of the first term and subsequent terms are much smaller. Neglecting the cubic and all subsequent terms of the series we have:

$$\alpha_e = \frac{2CL}{\pi(2 - C_L)} \qquad (10)$$

From Ref. 1 an expression for the spray thickness is given as follows:

$$\frac{\delta}{\ell} \cong \frac{\delta}{r} = \frac{\pi}{\frac{1+\cos\tau}{1-\cos\tau} - \ell n \frac{1-\cos\tau}{2\cos\tau} + \frac{\pi\sin\tau}{1-\cos\tau}} \tag{11}$$

Referring to Fig. 2, one notes that r is measured from the trailing edge to the stagnation point while ℓ is measured from the trailing edge to a line tangent to the spray root. The difference between r and ℓ is considered insignificant. If in equation (7) we now let $\tan\alpha_i \approx \alpha_i$, equation (8) becomes

$$\tau = \frac{2\,C_L}{\pi(2 - C_L)} + \frac{C_L + \dfrac{2\pi\sin\tau}{\frac{1+\cos\tau}{1-\cos\tau} - \ell n \frac{1-\cos\tau}{2\cos\tau} + \frac{\pi\sin\tau}{1-\cos\tau}}}{(\pi/2\lambda + 4\sin\tau)} \tag{12}$$

The following substitutions are made to simplify the algebra:

Let $$\frac{2\pi\sin\tau}{\frac{1+\cos\tau}{1-\cos\tau} - \ell n \frac{1-\cos\tau}{2\cos\tau} + \frac{\pi\sin\tau}{1-\cos\tau}} = A$$

and $$\left(\frac{\pi}{2\lambda} + 4\sin\tau\right) = B$$

Equation (12) then takes the form:

$$\tau = \frac{2C_L}{\pi(2 - C_L)} + \frac{C_L + A}{B}$$

Clearing fractions and collecting like powers of C_L we find:

$$C_L^2 - (B\tau + \frac{2}{\pi}B + 2 - A)C_L - 2(A - B\tau) = 0 \tag{13}$$

and solution by the quadratic formula yields:

$$C_L = \frac{B(\tau + \frac{2}{\pi}) + 2 - A}{2} \pm \sqrt{\left[\frac{B\tau + \frac{2}{\pi}B + 2 - A}{2}\right]^2 + 2(A - B\tau)} \tag{14}$$

To facilitate numerical calculations, one notes that A can be simplified considerably. Ref. 1 contains a numerically evaluated plot of

δ/r vs. τ. From zero to about 45 degrees, the curvature is slight so that a straight line approximation will not introduce material error in subsequent computations. The linearization is carried out by making the straight line coincide with the curve at zero and 25 degrees. The slope K of the straight line is then found per radian to be approximately 0.2 so that:

$$A = 2 \frac{\delta}{\ell} \sin \tau$$

becomes approximately

$$A \cong (2)\ (0.2)\tau^2 = 0.4\tau^2 \tag{15}$$

Values of A and B are tabulated in Table I, then the quadratic equation is solved. The values found from solution of equation (14) without linearizing δ/ℓ and those found when equation (15) was substituted for A show no appreciable difference; therefore, the values of A in Table I are those found using equation (15). Table II contains the numerical values of equation (14), and Fig. 3 is a plot of these values.

Modification of the two-dimensional flat-plate-airfoil solution for the low aspect ratio case by the method used here led to results which, compared with experimental data, overestimated the lift. Similarly, the planing results developed here overestimate experimental results.

Application of the Momentum Theorem - Method II

The fact that planing lift results are overestimated by the above development leads one rather logically to the conclusion that the virtual mass chosen was too large. Reflection upon the phenomena occurring at the plate then leads one to conclude that a new definition of

virtual mass based upon the ambient flow angle rather than the geometric angle of trim should be used.

Redefining the virtual mass, we obtain

$$L = \rho V b \ell \left(\frac{\pi}{8\lambda} + \sin\alpha_e\right) v_{i\infty} - \rho V^2 b\, \delta \sin\alpha_e \qquad (16)$$

Dividing by 2V, transposing, and simplifying as before, there results:

$$\frac{v_{i\infty}}{2V} = \tan\alpha_i = \frac{C_L + 2\frac{\delta}{\ell}\sin\alpha_e}{\left(\frac{\pi}{2\lambda} + 4\sin\alpha_e\right)} \qquad (17)$$

Substituting for $\sin\alpha_e$, the value found from the two-dimensional solution, we find:

$$\alpha_i = \frac{C_L + 2\frac{\delta}{\ell}\left[\frac{2C_L}{\pi(2 - C_L)}\right]}{\frac{\pi}{2\lambda} + 4\left[\frac{2C_L}{\pi(2 - C_L)}\right]}$$

Again substituting in equation (8) there is obtained:

$$\tau = \frac{2C_L}{2\pi - \pi C_L} + \frac{C_L + \frac{4\frac{\delta}{\ell}C_L}{2\pi - \pi C_L}}{\frac{\pi}{2\lambda} + \frac{8C_L}{2\pi - \pi C_L}} \qquad (18)$$

Simplification of equation (18) using the linearization for δ/ℓ as previously described leads to the cubic equation:

$$C_L^3 + \left[\left(\frac{8}{\pi} - \frac{\pi}{2\lambda} - \frac{4K}{\pi}\right)\tau - \frac{1}{\lambda} + \frac{16}{\pi^2} - 4\right]C_L^2$$
$$+ \left[\left(\frac{2\pi}{\lambda} - \frac{16}{\pi} + \frac{8K}{\pi}\right)\tau + \frac{2}{\lambda} + 4\right]C_L - \frac{2\pi}{\lambda}\tau = 0 \qquad (19)$$

Substitution of $\lambda = 0$ in equation (19) recovers the two-dimensional results.

Solutions for equation (19) are tabulated in Table III and plotted on Fig. 4.

The values of C_L obtained by this method underpredict the experimental values above values of λ of about 1.5 to 2. One may conclude then that the virtual mass selected in this manner is too small for the low aspect ratio case and too high for the large aspect ratio case. The low aspect ratio airfoil treatment by this method also underestimates the lift.

EXPERIMENTAL INVESTIGATION

Purpose

A comparison of experimental data with the results computed by the two formulas for the lift coefficient developed herein was undertaken. It soon became evident that existing published data did not cover the entire aspect ratio-angle of trim range desired; therefore, the necessary tests were performed in the towing tank to supply the otherwise unavilable data. To this end, the facilities of the seaplane tank at the Experimental Towing Tank, Stevens Institute of Technology were employed.

Equipment and Procedure

The model used for the tests was machined from half-hard brass bar stock, and provision for supporting the model in the towing carriage was made by mechanical linkages shown in Fig. 5. The overall length of the model was 18 inches, the beam 2 inches, giving the

general appearance of a rectangular ski. The lengthwise edges of the upper surface of the ski were beveled at an angle of 30 degrees as shown in the sketch of Fig. 5. The upper surface bevel provided sharp edges for a clean break-away of flow. The flat bottom which was the wetted surface during the tests was polished and marked with Dykem Steel Bluing to permit ease of reading the wetted lengths from the underwater photographs made during each test run. The marking details are also shown in Fig. 5. To eliminate the adverse effects of spray on the carriage, it was found that vertical separation between the model and carriage supporting linkages was necessary. To provide the required vertical separation, two mounting rods, approximately 3-1/4 inches long were tapped into the upper surface of the model near the after end.

The seaplane tank where the tests were conducted is 313 feet long, 12 feet wide, and 6 feet deep when the water level is just even with the opening in the standpipe inside the tank. A maximum carriage speed of 50 feet per second can be attained with the selected speed, amplidyne controlled, carriage driving motor. A tachometer generator, the armature of which is driven by the carriage driving motor shaft, supplies electrical information to the field of the amplidyne system to provide speed control. With a selected voltage, representing a certain speed, the carriage speed can be maintained to within 0.06 feet per second. A General Electric photoelectric tachometer records the carriage speed.

The camera for making underwater photographs of the wetted surface was a specially adapted Beattie Varitron, Model E, Data Recording Camera. The Varitron is a low speed, pulse type camera, the operation of which is completely automatic. An electrical signal operates the shutter of the camera, and as the shutter opens, it triggers the photoflood lights to make the exposure. Following the exposure, the shutter is automatically disconnected while another circuit provides power for winding the film in the magazine to the next frame. When film winding is completed, the shutter circuit is re-engaged, and the apparatus is ready to make another exposure. A recording chamber on the side of the camera automatically records sequence numbers and information on a platten to identify the test. The camera for the tests described herein was housed in a watertight box and pressurized to insure against leakage. A control for remote focusing after the camera had been positioned in the tank was also provided. A light source, mirror, photocell, and thyratron were used to actuate a relay which delivered the electrical pulse to the camera shutter.

The model was installed in the overhead towing carriage as shown in Fig. 5 with provisions made to set the angle of trim as desired. With the trim angle set at zero degrees, adjustments were made to insure that there was no angle of roll or yaw. By gently lowering the ski into the water and observing the bottom surface with a mirror held underwater below the ski, a simultaneous wetting of the entire bottom surface indicated proper alignment in roll. Yaw was checked by placing a bar with reference marks inscribed thereon at the front edge of

the ski, perpendicular to the direction of motion and in the plane of the bottom surface of the ski. Then, if by moving the carriage forward, the edge of the ski remained on the reference mark, yaw angle was considered zero. A spirit level protractor was used to set the angle of trim.

With the desired angle of trim set, a calibration in heave was made so that during the runs, a first order approximation on the wetted lengths could be ascertained. To accomplish the heave calibration, the ski was again gently lowered into the water and observations in the underwater mirror were made similar to those for the roll adjustment. When the trailing edge of the ski just touched the water, the heave reading was taken on the large scale as shown in Fig. 5. This reading was listed on the data sheet (Table IV of this report) as the heave reference, and this reference value was subtracted from the heave reading made during the run. The difference (or sum of absolute values in the case of a negative heave reference) gave the vertical projection of the wetted length of ski excluding the wave rise. Then by an empirical wave rise factor, described in Ref. 18, the approximate total wetted length could be found. Let it be emphasized here that the heave readings were used in the tests as a control measure only. Since there are wave disturbances in the tank after the first run, slight transient effects limit the accuracy of heave readings. The procedure for obtaining approximate wetted lengths from heave readings was as follows (see Fig. 6):

Let: $\frac{\ell_1}{b}$ = wetted length/beam ratio of the ski neglecting wave rise

h = difference in heave (running heave minus reference heave, inches)

$\frac{\Delta\ell}{b}$ = empirical wave rise factor = .3

τ = trim angle (degrees)

$\lambda = \ell/b$ = total wetted length/beam ratio

$$\frac{\ell_1}{b} + \frac{\Delta\ell}{b} = \frac{\ell}{b} = \lambda \qquad \frac{h}{b\sin\tau} = \ell_1/b$$

$$\lambda = \frac{\ell}{b} = \frac{h}{b\sin\tau} + .3 \qquad h = (\lambda - .3)(b\sin\tau)$$

Anticipating specified wetted lengths made it is possible to determine approximately the desired value of h so that during the runs, the values of h served as a check on actual wetted lengths being obtained. Adjustment of the load to get the desired value of h and, thus, the actual wetted length, was then practical.

In order to eliminate all effects of gravity on the lift coefficient obtained by the tests, all runs were made with a speed coefficient, C_V, at a nominal value of twelve. Theoretical justification for independence of gravitational effects on the total lift coefficient at high Froude Numbers will be treated later. (Refer to Fig. 7). Since the beam of the model was two inches, a carriage speed of 27.8 feet per second was found to be appropriate. (Note that $C_V = V/\sqrt{gb}$ or $V = C_V\sqrt{gb}$).

For each run, a pre-determined load was applied to the model which was allowed to run free in heave with a fixed angle of trim and

at constant speed. The wetted length for each run was photographed so that correlation with load could be made for data reduction.

Table IV, which is a copy of the laboratory data sheet, contains all of the information pertinent to each of the test runs. Table V, containing wave rise "correction" factors computed from the heave readings and the underwater photographs, was made as a check on the previous empirical wave rise factor and is intended to supplement present existing information for future tests which other investigators may perform in the aspect-ratio-angle of trim range covered herein.

Experimental Results

Reduction of experimental data from the photographs taken and carriage speeds recorded are found in Table VI.

Since most of the experimental data collected from the tests here were beyond the range of existing data, it was not possible to evaluate the reproducibility of such results, particularly in the limited time available. The general trend of curves faired through the test points obtained in this investigation is to lie between the curves of Fig. 3 and 4 which leads one to believe that the results are reasonable. It is noted from the ratios of computed values based on α_e to experimental values tabulated in Table VII and shown on Fig. 8 that the data collapses fairly well for trim angles of 18 degrees or less. Above 18° the dependence of experimental values of the lift coefficient upon the angle of trim manifests itself, but it is not clear

from a physical viewpoint just what the relationship between λ, τ, and C_L should be.

COMPARISON OF THEORETICAL RESULTS WITH EXPERIMENTAL DATA

General Discussion

In order to determine the validity of calculations made by correcting the two-dimensional planing solution for the effect of finite span, a comparison was made with experimental data. The principal source of data used was from Weinstein and Kapryan, Ref. 19. Since the existing data available did not cover the complete angle of trim, wetted length-beam ratio range desired, additional data were obtained experimentally and are presented herein. Of the several methods available for comparing data, it was decided that ratios of computed values to experimental values plotted against λ with τ as parameter would give the most enlightening results. Values of the ratios using both method 1 and method 2 previously described for computing values of C_L are found in Table VII and are plotted on Fig. 8 and 9. Since the ratios are not of the order of unity, it becomes necessary to make an empirical correction to the computed values in order to predict the lift coefficient satisfactorily.

Empirical Correction to the Curves of C_L Computed by the Cubic Equation

For $\dot{m}$ defined as a function of α_e, it is seen that as λ becomes greater than about 2, computed values of C_L from equation (19) underestimate the experimental values. The ratios of computed C_L to ex-

perimental C_L values found in Table VIII and plotted on Fig. 8 show that for trim angles of 18 degrees or less, the ratio plot tends to collapse into a single curve. For the case of C_L computed on the basis of equation (14) the plot of ratios, Fig. 9, does not collapse as neatly as the plot of Fig. 8. For this reason, empirical correction to the curves of C_L computed by equation (19) was elected.

The curve shown on Fig. 8 was faired to fit most of the points and the empirical factor found as follows:

$$\frac{\dfrac{C_{L\ computed}}{C_{L\ experimental}}}{\eta} = 1 \tag{20}$$

where η = empirical correction factor.

For $2^\circ \leqslant \tau \leqslant 18^\circ$, $\eta = f(\lambda)$ and we call this factor η_1. For $18^\circ \leqslant \tau \leqslant 30^\circ$, $\eta = f(\lambda, \tau)$ and this factor is denoted by η_2.

There are, of course, several suitable functions to fulfill the requirements on η, but the ones chosen here are:

$$\eta_1 = 1.359 - \tanh\ \left(\frac{1 + \lambda}{8}\right) \tag{21}$$

$$\eta_2 = \eta_1 + \frac{\Delta\tau}{1.58} \tanh\ \lambda^2 \tag{22}$$

From Fig. 8, the intercept value of the curve is recovered from η_1 when $\lambda = 0$.

In equation (22), $\Delta\tau$ is defined as $\dfrac{\tau^\circ - 18^\circ}{57.3}$ radians. Then when $\lambda = 0$, $\eta_1 = \eta_2$.

The empirical factors, η_1 and η_2, have been applied to values of C_L computed by equation (19) and the results tabulated in Table VIII. Fig. 10 is a plot of the empirically corrected values of C_L and is

the one to be used for estimating the lift coefficient when gravity is not considered.

Fig. 11 shows the empirically corrected curves of C_L vs. λ with experimental data points plotted thereon.

THE EFFECT OF GRAVITY

One can recognize that the influence of gravity in the case of a planing body can manifest itself in two separate ways. One part of the gravity contribution is a static force which is the Archimedian lift or buoyancy; the other is a dynamic effect which attends the phenomena of the development of waves.

Until recently, the effects of gravity on the dynamic lift have been practically ignored in planing lift calculations, partially because the mechanism of the dynamic effects has not been clearly understood (Ref. 5, 17, 20), and partially because the theory, including the dynamic effects, is quite complex and difficult to evaluate.

In 1937, L. I. Sedov, Ref. 2, presented a two-dimensional asymptotic solution to the planing problem, including the effects of gravity on the dynamic lift in the region of high Froude numbers. For more practical applications, Hajime Maruo, Ref. 3, published in 1951 a two-dimensional solution to the planing problem, and followed this in 1953, Ref. 21, with a solution for the finite span.

It is considered appropriate to summarize here the Maruo paper, Ref. 21, which reveals the effects of gravity on the lift of the planing flat plate of finite span.

Maruo assumes a form for the velocity potential function ϕ which involves an unknown pressure distribution over the planing surface.

$$\phi = \frac{i}{4\pi^2 \rho U} \int\int_{-\infty}^{\infty} d\alpha \, d\beta \iint_S \frac{\alpha e^{i\{\alpha(x-\xi)+\beta(y-\eta)\}+\sqrt{\alpha^2+\beta^2}\,z}}{\alpha^2 - K\sqrt{\alpha^2+\beta^2} + i\mu\alpha} p_s(\xi,\eta)\, d\xi \, d\eta$$

This potential function is constructed to satisfy the free surface condition of constant pressure except on the planing surface. Then, from the potential function, a general formula for the downwash is found.

$$w = \lim_{\substack{z \to 0 \\ \mu \to 0}} \frac{i}{4\pi^2 \rho U^2} \iint_S p_s(\xi,\eta)\, d\xi \, d\eta \int_{-\pi}^{\pi} \sec\theta \, d\theta \int_0^{\infty} \frac{e^{kz + ik\{(x-\xi)\cos\theta + (y-\eta)\sin\theta\}}}{k - K\sec^2\theta + i\mu\sec\theta} k^2 \, dk$$

Maruo points out that the downwash can be separated into two components; one corresponds to a profile characteristic and is present even in the two-dimensional flow; the other is a downwash arising from the effect of finite span.

The downwash condition applied at the planing surface to satisfy the condition of no flow through the plate, gives rise to an integral equation for the unknown pressure distribution over the plate.

Maruo, by a procedure analogous to Glauert's solution of the finite span airfoil problem, simplifies and solves the integral equation for values of $\lambda \leq 1/2$, or for aspect ratios greater than about two. Fig. 7 is a graphical representation of the solution when $\lambda \to 0$.

One should note on Fig. 7 that there are two curves, I and II. Curve I is the plot of a numerical solution to the exact equation while II is a plot of the simplified equation evaluated analytically. Attention is directed to the shape of the curve of Fig. 7 which shows

that the theoretical value of C_L, not considering buoyancy effects, rises from a C_V of 0.75 and approaches asymptotically a constant value at higher C_V. Most plots of experimental data show the total lift coefficient without subtracting the coefficient of buoyancy $B/\frac{1}{2}\rho V^2 b\ell$ from the data; therefore, the effect of gravity on the dynamic lift appears to be a monotonically decreasing function of C_V rather than an increasing function as shown by the theory.

The practical results of Maruo's work are given by Equation (42) of Ref. 21 which, when transcribed to the notation used herein, becomes:

$$C_L = \frac{\tau}{\lambda\psi + \frac{1}{3}}$$

where ψ is a function of the speed coefficient, C_V.

A graph of the ψ function, given in Ref. 21, can be linearized to the following approximation:

$$\psi = 0.667 + \frac{0.233}{C_V^2}.$$

Then C_L becomes:

$$C_L = \frac{\tau}{0.667\lambda + 0.333 + \frac{0.233\lambda}{C_V^2}} \qquad (23)$$

From equation (23), it is evident that the lift coefficient becomes independent of the dynamic effects of gravity for

$$C_V > \sqrt{\frac{0.7\lambda}{1 + 2\lambda}}$$

One should be aware of the fact that the mathematical validity of equation (23) was based on $\lambda \leq 1/2$.

For small λ (such that $2\lambda << 1$), it is seen that the first term of the binomial expansion of the inequality yields $C_V > 0.6\sqrt{\lambda}$ which agrees quite well with the empirical value of $C_V/\sqrt{\lambda} > 1$ established by Daniel Savitsky, Ref. 18, as a criteria for independence of gravity in the flow.

The effect of gravity on the dynamic lift from this analysis is seen to become negligible at low values of C_V. Those investigators who insist that the value of C_V above perhaps 10 is necessary to eliminate the gravity effect refer to the combined buoyant and dynamic effects. The dynamic effects become small at low values of C_V, but until the dynamic pressure, $1/2\,\rho V^2$, becomes large enough to make the ratio of static buoyant force to dynamic pressure a small percentage of the total lift, buoyant effects will persist.

For most practical cases, the lift coefficient, as C_V approaches the order of 10, is clearly independent of all gravity effects. If one subtracts from the total lift coefficient the buoyant lift contribution defined by $\frac{B}{1/2\,\rho V^2 b\ell}$, it is seen that the remainder is independent of all effects of gravity only for $C_V > 0.6\sqrt{\lambda}$ when $\lambda \leq 1/2$.

SUMMARY AND CONCLUSIONS

The results of this investigation show that theoretical evaluation of the effect of a finite span on the planing surface problem is quite complex. To remove some of the complexity, the problem was considered in two phases. First, the effects of gravity were neglected, and an ideal fluid assumed; then second, the effects of gravity were discussed.

Neglecting gravity, equation (14) was obtained from a combination of the two-dimensional solution and application of the momentum theorem to a selected virtual mass. Equation (19) was found in a similar manner but with a different virtual mass. Both equations (14) and (19) overestimate the lift coefficient for aspect ratios greater than about one-half which indicates that the choice of virtual mass for that range of aspect ratios is too high. Equation (19) underestimates the lift when wetted length-beam ratios are greater than about two (aspect ratio less than one-half), while equation (14) overestimates the lift for all length-beam ratios.

Fig. 1 shows cross-sectional areas of the "volumes" containing the virtual mass for each case. Tables II and III give tabulated values of the calculations made by each of the above methods, and Table VIII gives the empirical corrections to make values computed by equation (19) agree with experimental data. Empirically corrected values of the lift coefficient are plotted on Fig. 10, and comparison of these curves with experimental data are shown on Fig. 11.

While the analytical results obtained are considered reasonable, empirical correction to the theoretical analysis was required to get better agreement with experimental data. Thus, the development can be considered as a semi-empirical method for evaluating the effect of a finite span on the solution to the planing problem in a weightless fluid.

For the analysis made independent of gravity at length-beam-ratios greater than about 2, the method leading to equation (19)

indicates that the virtual mass may be too small. The virtual mass associated with equation (14) may be too large. The most prominent physical explanation for the inconsistency between theoretical and experimental results is that the downwash along the wetted length of the body is not of constant magnitude. Bollay, Ref. 16, indicates that free vortex lines are shed along the chord of the low aspect ratio airfoil so that at the trailing edge, the contribution to downwash there is not only from the vortex wake, but also from the shed vorticity ahead. This, in effect, produces a curvature of the flow from leading to trailing edge which has the effect of introducing an apparent camber to the foil.

For the low aspect ratio (large λ) planing surface, the curvature effect may have a significant influence on the lift, and is offered as a possible explanation for the difference between predicted and experimental values.

It is worthy of notice here that the technique similar to that used for modifying the infinite span airfoil for the effect of finite span is a logical procedure to use for the planing surface. As pointed out by many other investigators, the flow for most practical purposes can be considered ideal and weighless in the planing regime, and from the stagnation point to trailing edge on the lower surface, both airfoil and planing body have almost identical pressure distributions.

The consideration of gravity led to results which show that the effect of gravity on dynamic lift is a function of the speed coefficient

and the wetted length-beam ratio. It was found that for all practical purposes, the effect of gravity on dynamic lift could be disregarded for $C_V > 0.6\sqrt{\lambda}$ when $\lambda < 1/2$. Buoyant effects remain significant until the dynamic pressure reaches such a value as to make the coefficient of buoyancy very small compared with the dynamic lift coefficient.

BIBLIOGRAPHY

1. Korvin-Kroukovsky, B. V.: Hydrodynamic Design of Seaplanes II, Experimental Towing Tank, Stevens Institute of Technology, Hoboken, N.J. (Summary of the applicable work of H. Wagner included).

2. Sedov, L.I.: Two-Dimensional Problem of Planing on the Surface of a Heavy Fluid, Unpublished Translation by B.V. Korvin-Kroukovsky, Experimental Towing Tank, Stevens Institute of Technology, Hoboken, N.J., 1937.

3. Maruo, Hajime: Two-Dimensional Theory of the Hydroplane, Proceedings of the First Japan National Conference for Applied Mechanics, 1951.

4. Korvin-Kroukovsky, B.V.: Lift of Planing Surfaces, Journal of Aeronautical Science, (Readers' Forum), Vol. 17, No. 9, September 1950, pp. 597-599.

5. Perry, Byrne: The Effect of Aspect Ratio on the Lift of Flat Planing Surfaces, Report No. E-24.5 (Contract N6onr-24424, Project NR 234-001), Hydrodynamics Lab., California Institute of Technology, September 1952.

6. Perry, Byrne: The Lift of Flat Planing Surfaces, Preliminary Report No. N-31.3, Hydrodynamics Laboratory, California Institute of Technology, March 1950.

7. Bollay, William: A Contribution to the Theory of Planing Surfaces, Proceedings Fifth Int. Cong. Appl. Mech. (Cambridge, Mass., 1938), John Wiley and Sons, Inc., 1939, pp. 474-477.

8. Perring, W.G.A. and Johnston, L.: The Hydrodynamic Forces and Moments on Simple Planing Surfaces, and an Analysis of the Hydrodynamic Forces and Moments on a Flying-Boat Hull, R & M No. 1646, British Aeronautical Research Committee, 1935.

9. Sottorf, W.: Analysis of Experimental Investigations of the Planing Process on the Surface of Water, NACA T.M. No. 1061, 1944.

10. Landweber, L. and Eisenberg, P.: Characteristic Curves for Planing Surfaces, David Taylor Model Basin Report R-80, 1943.

11. Locke, F.W.S., Jr.: An Empirical Study of Low Aspect Ratio Lifting Surfaces with Particular Regard to Planing Craft, NAVAER DR Report No. 1043, January 1948.

12. Shuford, C.L., Jr.: A Review of Planing Theory and Experiment with a Theoretical Study of Pure Planing Lift of Rectangular Flat Plates, NACA T.N. 3233, Langley Aeronautical Laboratory, August 1954.

13. Siler, William: Lift and Moment of Flat Rectangular Low Aspect Ratio Lifting Surfaces, Experimental Towing Tank Technical Memorandum No. 96, Unpublished, 1949.

14. Weinig, F.: Lift and Drag of Wings with Small Span, NACA T.M. No. 1151, August 1947.

15. Munk, Max M.: Fundamentals of Fluid Dynamics for Aircraft Designers, The Ronald Press Co., New York, 1929.

16. Bollay, William: A Theory for Rectangular Wings of Small Aspect Ratios, Journal of Aeronautical Sciences, Vol. IV, No. 7, May 1937.

17. Weinig, F.: On the Theory of Hydrofoils and Planing Surfaces, NACA T.M. No. 845, January 1938.

18. Savitsky, Daniel and Neidinger, Joseph W.: Wetted Area and Center of Pressure of Planing Surfaces at Very Low Speed Coefficients, Experimental Towing Tank, Stevens Institute of Technology, a Sherman M. Fairchild Publication Fund Paper by the Institute of Aeronautical Sciences, Deptember 1954, No. FF-11.

19. Weinstein, Irving and Kapryan, Walter J.: The High Speed Planing Characteristics of a Rectangular Flat Plate Over a Wide Range of Trim and Wetted Length, NACA T.N. 2981, Langley Aeronautical Laboratory, July 1953.

20. Wagner, H.: Planing of Water Craft, NACA T.M. No. 1139, April 1948.

21. Maruo, Hajime: Theory of the Hydroplane with Broad and Short Planing Surfaces, Bulletin of the Faculty of Engineering, Yokohama National University, Yokohama, Japan, Marcy 1953.

22. Milne-Thomson, L.M.: Theoretical Aerodynamics, MacMillian Co., Inc., New York, May 1947.

23. Perelmuter, A.: On the Determination of the Take-Off Characteristics of a Seaplane, NACA T.M. No. 863, May 1938.

24. Winter, H.: Flow Phenomena on Plates and Airfoils of Short Span, NACA T.M. 798, 1936.

25. Lawrence, H.R.: The Lift Distribution on Low Aspect Ratio Wings at Subsonic Speeds, Journal of Aeronautical Sciences, Vol. 18, No. 10, October 1951.

APPENDIX I

General

The use of incompressible potential flow theory to treat the effects of low aspect ratio on wing lift has been carried out for the case of a flat plate airfoil in at least two distinctly different ways, but with essentially the same result. The two different methods cited are:

(1) The solution by F. Weinig, Ref. 14, whereby the momentum theorem is applied with an estimate of virtual mass, and an estimate for the induced angle of attack, α_i, is made based on cascade theory.

(2) The integral equation solution of W. Bollay, Ref. 16, in which the boundary condition—that there be no flow through the plate—is satisfied by equating the transverse velocity component of the stream, $V \sin\alpha$, to an integral expression established for the downwash at the wing.

It should be noted that both of these methods are developed for an airfoil in an incompressible fluid neglecting gravity; therefore, it is reasonable to expect the results to be analogous to that portion of the planing problem which is treated independent of gravity. Wagner, Perlemuter, Perry, and Shuford, Ref. 1, 5, 6, 12, 20, and 23, have indicated that the integral of pressures over the wetted surface of the planing body, excluding the region about the leading edge forward of the stagnation point, is almost identical with the pressure distribution over the same portion of a flat plate airfoil;

thus, the planing surface-airfoil analogy seems to be reasonably founded.

It is not the purpose of this discussion to present the details of the airfoil solutions of Weinig and Bollay, but rather to show how they lead to a better understanding of the virtual mass chosen to modify the two-dimensional planing surface solution for the effect of a finite span. The fact that the solutions of both Weinig and Bollay lead to essentially the same result is graphically revealed in Fig. 12. The experimental points shown in Fig. 12 were obtained by H. Winter, Ref. 24, and are included to show the relative merit of each of the theoretical results displayed. One obvious reason for the difference between the theoretical solutions of Weinig and Bollay is that mathematical complexity forced Bollay to make several simplifying assumptions in order to solve the integral equation established in his formulation of the problem. Although Bollay's treatment of this problem seems to be established on a more rational foundation, Weinig's results correlate better with experimental data as pointed out by H.R. Lawrence, Ref. 25.

Virtual Mass

Modification of the two-dimensional planing surface problem for the effect of a finite span by application of the momentum theorem makes necessary the choice of an appropriate virtual mass. Attention is directed to the low aspect ratio airfoil solution by Weinig wherein the virtual mass selected is composed of the virtual mass associated

with a lifting line plus the streamwise projection of the chord $b\ell \sin \alpha$. In order to better understand Weinig's choice of virtual mass, a review of the salient features of the virtual mass concept as given by M.M. Munk, Ref. 15, are considered. A brief review of the most important steps leading to the definition of virtual mass follows.

If an incompressible fluid at rest is given an impulse which results from the action of normal pressures alone (frictional forces assumed zero) the resulting flow is potential flow provided no discontinuities exist and all spacewise partial derivatives of the potential function are continuous. If it is assumed that the impulsive force creating the flow acted for some finite distance, work would be done on the fluid, and since the fluid was originally at rest with zero kinetic energy, the work done represents the kinetic energy stored in the flow. It is convenient to replace the total energy of the fluid particles moving in many different directions with the equivalent energy of a certain geometrically defined mass of the fluid moving with the velocity of the body. This assumed mass, introduced for mathematical convenience, is labeled virtual mass and may be different in magnitude for different directions, depending on the velocity chosen in its definition.

If a very thin airfoil with axes fixed in the body moves with a steady velocity in air which was originally at rest, velocity about the airfoil at angle of attack, α, can be resolved into two components, one normal and one parallel to the foil as shown in the sketch.

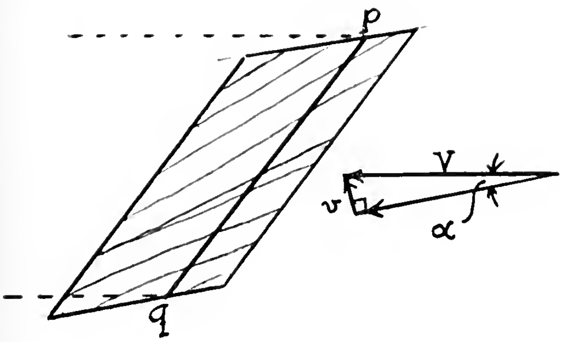

In an ideal fluid (no friction), the component parallel to the airfoil does not contribute to the forces. Attention is then concentrated on the normal component which is referred to as the transverse flow component. The line pq on the sketch represents an element of the airfoil of span b. (It has been shown that when the span to chord ratio is large, the entire foil may be represented by such a line.) The wake at some distance behind this airfoil behaves like a flat plate of span b moving with velocity v perpendicular to the plane described by the plate. The complex potential for the flow net about this hypothetical flat plate is given by:

$$w = \phi + i\psi = iv\left(z - \sqrt{z^2 - \left(\frac{b}{2}\right)^2}\right) \qquad \text{(A1-1)}$$

where $z = x + iy$, v = transverse velocity component, and $b/2$ = semi-span. The product, $\rho\phi$, can be thought of as the impulsive pressure necessary to create the flow field in which kinetic energy is stored. Then, the expression for kinetic energy in terms of the potential function is:

$$T = 1/2 \int \rho\, \phi \, \frac{d\phi}{dn}\, ds \qquad \text{(A1-2)}$$

where ρ = fluid density

$d\phi/dn$ = component of transverse flow velocity

ds = surface element over which the integral is performed.

This is the total kinetic energy of the flow, and as previously

stated, it can be expressed in terms of the virtual mass, m, as

$$T = 1/2\ mv^2 \tag{A1-3}$$

where $v = d\phi/dn$ = constant on the surface of the plate. The total kinetic energy of the flow as found by the potential function is equated to the energy expressed by the virtual mass so that

$$\frac{1}{2}\int_S \rho \phi \frac{d\phi}{dn} ds = \frac{1}{2} mv^2 \tag{A1-4}$$

Since ρ = constant and $\left. d\phi/dn \right]_{\text{plate}} = v$ = constant, there is obtained:

$$\text{Vol} = \frac{1}{v^2}\int_S \phi \frac{d\phi}{dn} ds \tag{A1-5}$$

This defines the volume of fluid of density ρ associated with the transverse velocity. It should be noted that the virtual mass is not a physical body of particles; its properties, as stated previously, are directional such that for a direction other than that of the transverse flow, the virtual mass may be entirely different.

On the surface of the hypothetical plate (i.e. y = 0 in the complex variable notation):

$$\phi = v\sqrt{\frac{b}{2}^2 - x^2} \tag{A1-6}$$

Substituting the value of ϕ from equation (A1-6) into equation (A1-5), and noting that $d\phi/dn$ is constant over the plate equal to v, the volume of fluid defining the virtual mass is obtained:

$$\text{Vol} = \int_S \sqrt{\frac{b}{2}^2 - x^2}\, dx \tag{A1-7}$$

Since the surface over which the integral is performed extends from -b/2 to +b/2 on both upper and lower surfaces of the plate, the final expression for the volume becomes

$$\text{Vol} = 2\int_{-b/2}^{b/2} \sqrt{\frac{b}{2}^2 - x^2}\, dx = \frac{\pi b^2}{4} \tag{A1-8}$$

This is the volume of fluid containing the virtual mass and is shown here to correspond to the mass of a circular cylinder of diameter equal to the span of the plate.

The Lifting Line

In the previous derivation of lift over the span b and an element of length $d\ell$, the downwash velocity, $v = d\phi/dn$ was necessarily constant along the span and was assumed to have no chordwise variation. The same constant downwash velocity is known to exist in the case of the vortex system consisting of bound and trailing vortices such that the circulation of the bound vortex varies elliptically along the span. The bound vortex is known as the Lifting Line, and it can be taken to represent the entire wing when the ratio of span to chord is large.

For multiple lifting lines disposed vertically in close proximity to each other, Munk has indicated that the interference existing between the flow patterns associated with each line reduces the virtual mass of the single line. The mathematical complexity involved for the case of three or more lines limits the discussion here to only qualitative, order of magnitude results.

In the case of a biplane, two lifting lines separated by a small vertical distance, h, can be assumed to replace the wings. The resulting volume containing the virtual mass associated with the transverse flow is given by Munk as approximately the cylinder of diameter equal to the span plus the rectangular mass enclosed between the upper

and lower wings:

$$\text{Vol} = \frac{\pi b^2}{4} + bh$$

The Effect of a Long Chord

The virtual mass associated with the lifting line, used in application of the momentum theorem to find the lift for a finite span airfoil leads to the prediction of reasonable values for span to chord ratios which are large. As the chord lengthens with respect to the span, the single lifting line representation becomes invalid, principally due to the fact that the free vortex lines no longer leave the trailing edge in a flat plane of the main stream, but instead are shed along the chord forward of the trailing edge to form a three-dimensional vortex array in the wake.

In order to satisfy the boundary conditions $d\phi/dn = V \sin\alpha$ on the surface of the airfoil, and of the streamlines flowing smoothly off the trailing edge, Bollay, Ref. 16,22, has assumed a distribution of bound vortex lines along the chord. After certain simplifications, Bollay has solved the integral equation for the distribution of circulation among these vortex lines (or lifting lines).

Interpreting Bollay's results in terms of virtual mass, the chordwise spacing of any pair of bound vortex lines at a distance $d\ell$ apart leads to an equivalent vertical spacing of $d\ell \sin\alpha$. Considering this in the light of Munk's theory of the biplane and multiple lifting lines, the integral along the chord of the contributions of all vortex pairs gives the contribution $b\ell \sin\alpha$ to the volume of the virtual mass as an approximation. The total volume associated with

an airfoil of small span and long chord then becomes $\frac{\pi b^2}{4} + b\ell \sin\alpha$. It is observed that this is the exact expression chosen by Weinig. It should be noted, however, that α in this case needs an interpretation. Weinig has assumed it to be equal to the geometric angle of attack of the airfoil, but in the spirit of the above derivation, it would appear more logical to use the ambient flow angle in the immediate vicinity of the airfoil rather than the geometric angle of flow.

Modification of the two-dimensional airfoil solution, using the momentum theorem, with the virtual mass based on geometric angle of attack, then on the ambient flow angle, follows.

Modification of the Two-Dimensional Airfoil Lift Coefficient for the Effect of Finite Span

Method 1 - virtual mass based on geometric angle of attack, α.

From the momentum theorem:

$$L = \dot{m}\, v_{i_\infty} = \frac{\rho V b \ell}{\lambda}\left(\frac{\pi}{4} + \lambda \sin\alpha\right) v_{i_\infty} \qquad \text{(A1-9)}$$

where $\dot{m} = \left(\frac{\pi b^2}{4} + b\ell \sin\alpha\right)\rho V$

$\lambda = \frac{\ell}{b}$

From energy relationships:

$$\frac{v_{i_\infty}}{2V} = \tan\alpha_i \approx \alpha_i \qquad \text{(A1-10)}$$

Dividing (A1-9) by 2V, substituting the result of (A1-10) and solving for α_i, there is obtained:

$$\alpha_i = \frac{\lambda L}{(2V)(\rho V b \ell)\left(\frac{\pi}{4} + \lambda \sin\alpha\right)} = \frac{\lambda C_L}{\pi + 4\lambda \sin\alpha} \qquad \text{(A1-11)}$$

where $C_L = \dfrac{L}{\frac{1}{2}\rho V^2 b\ell}$.

Now:

$$\alpha = \alpha_e + \alpha_i \tag{A1-12}$$

and from two-dimensional theory:

$$C_L = 2\pi \sin\alpha_e \cos\alpha_e \tag{A1-13}$$

Dividing (A1-13) by π:

$$\frac{C_L}{\pi} = 2 \sin\alpha_e \cos\alpha_e = \sin 2\alpha_e \tag{A1-14}$$

$$2\alpha_e = \text{arc sin } \frac{C_L}{\pi} \tag{A1-15}$$

Writing the series expansion for arc sin $\dfrac{C_L}{\pi}$:

$$\alpha_e = \frac{1}{2}\left\{\frac{C_L}{\pi} + \left(\frac{C_L}{\pi}\right)^3 \frac{1}{6} + \ldots\right\} \tag{A1-16}$$

Neglecting all terms in the series higher than the cubic, and substituting from (A1-16) and (A1-11) into (A1-12):

$$\alpha = \frac{1}{2}\left\{\frac{C_L}{\pi} + \left(\frac{C_L}{\pi}\right)^3 \frac{1}{6}\right\} + \frac{\lambda\, C_L}{\pi + 4\lambda \sin\alpha} \tag{A1-17}$$

Solving:

$$C_L^{\,3} + \left\{6\pi^2 + \frac{12\pi^3\lambda}{\pi + 4\lambda \sin\alpha}\right\} C_L - 12\pi^3\alpha = 0 \tag{A1-18}$$

Values of α substituted into (A1-18) show no appreciable difference from the results obtained as follows.

In equation (A1-13) let:

$$\cos\alpha_e \approx 1$$

$$\sin\alpha_e \approx \alpha_e$$

Then (A1-13) becomes:

$$C_L = 2\pi\alpha_e \tag{A1-19}$$

Multiplying (A1-12) by 2π, then substituting from (A1-11) and (A1-19), there is obtained:

$$2\pi\alpha = C_L + \frac{2\pi\lambda C_L}{\pi + 4\lambda \sin\alpha} \qquad \text{(A1-20)}$$

Equation (A1-20) simplifies to:

$$C_L = \frac{2\pi\alpha}{1 + \dfrac{2\pi\lambda}{\pi + 4\lambda \sin\alpha}} \qquad \text{(A1-21)}$$

Values of C_L computed by (A1-21) are tabulated in Table IX and plotted on Fig. 13. It is observed that this method overestimates the experimental values of Winter.

<u>Method 2</u> - virtual mass based on ambient flow angle, α_e. Similar to method 1, there is obtained for α_i:

$$\alpha_i = \frac{\lambda C_L}{\pi + 4\lambda \sin\alpha_e} \qquad \text{(A1-22)}$$

Approximating again:

$$\cos\alpha_e \approx 1$$

$$\sin\alpha_e \approx \alpha_e$$

and substituting $\alpha_e = \dfrac{C_L}{2\pi}$ in the equation:

$$\alpha = \alpha_e + \alpha_i$$

there is obtained:

$$\alpha = \frac{C_L}{2\pi} + \frac{\lambda C_L}{\pi + 4\lambda\alpha_e} = \frac{C_L}{2\pi} + \frac{\lambda C_L}{\pi + 4\lambda \dfrac{C_L}{2\pi}} \qquad \text{(A1-23)}$$

Simplifying and collecting coefficients of like powers of C_L:

$$C_L^{\,2} + \left\{\frac{\pi^2}{2\lambda} + \pi^2 - 2\pi\alpha\right\} C_L - \frac{\pi^3\alpha}{\lambda} = 0 \qquad \text{(A1-24)}$$

Equation (A1-24) is solved by the quadratic formula, values tabulated in Table IX and plotted on Fig. 13 for comparison with method 1 and the experimental data of Winter. It is observed that C_L is underestimated by equation (A1-24).

APPENDIX II

Foundations of the Theory of Planing

Translation of Paragraph 75 of the Russian Textbook, Water Resistance to Movement of Ships, by P. A. Apuchtin and J. I. Voitkunsky, Moscow, 1953.

The viscosity of a fluid affects the pressure distribution along the planing surface very little and separation of the boundary layer is not observed on planing surfaces. This provides the basis for investigation of the phenomena of planing by methods of hydrodynamics of a perfect fluid, in particular the potential flows.

In the domain of the theoretical investigation of planing, the Soviet scientists played a leading part. In 1929, G. E. Pavlenko first obtained the solution for the lifting force and resistance of a plate of infinite span, planing at a small angle of trim on the surface of a perfect fluid.

Later, G. E. Pavlenko developed the foundations of the theory of planing, taking into account the finite span, studied the physical phenomena connected with planing, and also investigated the question of recalculation of model test results of planing surfaces to full size.

In subsequent works, the two-dimensional problem of planing of plates on the surface of a perfect fluid was attacked along two paths:

1) by the methods of streamline flows, not taking into account the weight of the fluid,

2) by methods of the theory of waves of small height taking into account the weight of the fluid.

The investigations of planing by means of streamline flows for infinite depth and for finite depth of a fluid were conducted by the academicians S. A. Chaplygin, M. I. Gurievich, A. P. Yampolsky and Wagner.

The solutions of the planing problem of a curved plate, taking into account the weight of the fluid were given by the academicians N. E. Kotchin and L. I. Sedov.

The planing of the surfaces moving one after another (in tandem), interesting in connection with the action of steps, for the case of gravity-less fluid was investigated by L. I. Sedov.

Let us consider the origin and the calculation of water resistance for the planing flat plate on the surface of a perfect fluid.

Large pressure gradients are observed along the lower surface in the movement of the plate. Plots of the pressure distribution, measured experimentally along the centerline of the plate and along its edges at various angles of trim, are shown on Fig. 134.(1) Along the span of the plate pressure changes are not significant, while normal to the span in the region of the leading edge the pressure gradient is very large. A large drop of pressure is observed at the lateral edges, where the pressure abruptly drops to a value corresponding to the pressure in the undisturbed fluid.

In regions of large pressure gradient (in the regions of intersection with the free water surface), spray jets are formed. The pro-

(1) See Fig. 14

jection of the reaction of the jet, in the direction opposite to the direction of the plate movement, represents spray resistance.

Let us consider the flow of a parallel stream of velocity V onto a stationary plate. Consider the depth of the fluid limited, equal to h. The influence of gravity on the flow of the fluid will be neglected.

Flow of the fluid in such a motion is steady. Applying Bernoulli's equation to the particles on the free surface (Fig. 135),[1] and taking into account the fact that pressure on the free surface is constant, it can be shown that the velocity along the surface of the jet is constant also, and is equal to V.

In the actual motion of the plate, the velocity in the jet is double that of the plate motion. Isolate by means of a control surface the closed volume of the fluid ABCDEF.[1] According to the law of momenta, the flow of momenta through the control surface is equal to the vector of external forces applied to the volume, ABCDEF.

The difference of momenta flow through the sections of the control surface, AB and CD, is equal to VQ, where Q is the mass flow in the spray jet.

Projecting the flow of momenta through the control surface ABCDEF and the vector of forces applied to the plate on the axis OX, we get

$$R_x = \rho VQ\ (1+\cos\alpha)$$

and the total reaction is directed normal to the plate and is equal to

$$R = \frac{R_x}{\sin\alpha} = \rho VQ\ \frac{1+\cos\alpha}{\sin\alpha} = \rho VQ\ \mathrm{ctg}\,\frac{\alpha}{2}$$

(1) See Fig. 14

These formulae are valid for any value of the angle α; the theory discussed can be considered therefore as the non-linear theory of planing.

As the fluid velocity in the spray jet in the case of a stationary plate is equal to V, the volumetric flow is

$$Q = V\delta$$

where δ is the thickness of the spray.

The force, R_x, in the case considered is equal to the spray resistance, R_δ of the plate. Finally, the formulae for computation of the spray resistance and total hydrodynamic reaction in planing on the surface of a gravity-less fluid of arbitrary length at any angle of trim will take the following form:

$$R_\delta = \rho V^2 \delta \ (1+\cos\alpha) \tag{136}$$

$$R = \rho V^2 \delta \ \mathrm{ctg}\ \frac{\alpha}{2} \tag{137}$$

If the plate of infinite span planes on the surface of a fluid, located in the field of gravity, waves are formed in its wake. In this case, the additional force of wave resistance will act on the plate.

In the case of the motion of a planing plate on the surface of a perfect fluid, therefore, the total resistance is the sum of spray-making resistance, R_δ, and of the wave resistance, R_B. Considering formula (135)[1] in the light of the above derivation, we find that $R_B + R_\delta = D \tan\alpha$.

(1) $R_x = D \tan\alpha + R_{tp}$ (135)

D = total lift, i.e. dynamic + Archimedian

R_{tp} = the force of friction

The sum of forces $R_B + R_\delta$ represents the projection of the resultant force of normal pressures, distributed along the plate, onto the direction of motion, i.e. represents resistance due to pressures.

With the growth of relative velocity, the part played by the gravity forces diminishes in comparison with inertial forces; therefore the part played by wavemaking resistance in the total resistance of the plate diminishes.

The comparison of the relative importance of the wavemaking and spray resistance in the total resistance of the planing of the flat plate is given on Figure 136.[1]

The complicated calculations permitted L. I. Sedov to obtain the formula for computation of the ordinates of the free fluid surface, hydrodynamic pressure, lifting force, resistance and the hydrodynamic moment acting on the planing surface.

In cases of large relative velocities (small values of the parameter $\nu = \frac{1}{2\,Fr^2}$), the formula for calculation of the lifting force, resistance, and hydrodynamic moment of the flat plate were obtained by means of Sedov's theory:

$$R = R_z = \rho\pi(1 - \pi\nu - 4\nu/\pi)a\,V^2\alpha \qquad (138)$$

$$R_x = R\alpha \qquad (139)$$

$$M = \frac{\rho\pi}{2}\left(1 - \frac{8+3\pi^2}{3\pi}\right)a^2V^2\alpha \qquad (140)$$

where $a = \frac{\ell}{2}$ and $F_r = V/\sqrt{g\ell}$.

These formulae show that at the large relative velocities and small angles, α, the lifting force and hydrodynamic moment in planing

(1) See Fig. 14

are linear functions of the angle of trim.

More accurate numerical calculations of the lifting force and moment by Sedov's theory were made by U. S. Chaplygin for a large variation in the parameter, ν. Results of these calculations are compared on Fig. 137[1] with results computed by formulae (138) and (140). On Fig. 137(a) and (b) are plotted the dependence of C_z/α and the relative distance of the center of pressure from the rear edge of the plate ℓ_d/ℓ on the number Fr. = $v/\sqrt{g\ell}$. Comparison of the curves shows that beginning with Fr. = 2.8, i.e. with $\nu = 0.064$, the results of the refined numerical computations and of calculations by approximate formula coincide. In the case of very large Froude numbers, Fr., it can be assumed that $\nu \cong 0$; this assumption means physically that the gravity of the fluid is not considered. With the introduction of such an assumption, the formulae for the flat plate are further simplified to:

$$R = R_z = \rho\pi a\, V^2\alpha \tag{141}$$

$$R_x = \rho\pi a\, V^2\alpha^2 \tag{142}$$

$$M = \frac{1}{2}\rho\pi a^2 V^2\alpha \tag{143}$$

Were the distance of the center of pressure from the trailing edge of the plate computed by means of the above formula for the moment, it would be found that $\ell_d = (3/4)2a$ (i.e. $m_D = .75\lambda$); this agrees well with test results.

Let us compare formula (141) and (142) with the formulae for the computation of corresponding quantities obtained in the wing theory for a flat plate of infinite span in a streamline flow at small angles

(1) See Fig. 14

of attack:

$$R_z = 2\rho\pi a V^2\alpha \tag{144}$$

$$M = \rho\pi a^2 V^2\alpha \tag{145}$$

The flat plate represents the simplest wing. The comparison of these formulae shows that in planing at large Froude numbers the lifting force and moment of the plate is half that obtained in the flow around the plate deeply submerged in a fluid. This relationship points to the analogy of the flow on the lower part of the plate in both cases.

The development of the analogy between the planing surface and the wing has permitted application of a number of relationships obtained in wing theory to study the phenomena of planing.

From the theory of the wing it is known that in a flow about a plate at an angle of attack α, in accordance with the theorem of Joukowsky, a lifting force occurs, normal to the direction of the flow at infinity. The velocity at the trailing edge of the plate has a finite value, and the streamlines flow off smoothly. At the sharp leading edge the velocity tends to become infinite, and in connection with this, the pressure in the vicinity of the leading edge drops sharply. Hydrodynamic pressures are normal to the surface of the plate, and their resultant, $\overline{P}$, is also directed along the normal to the plate (Fig. 138,a).(1) In addition to the force $\overline{P}$, a suction force, $\overline{S}$, acts in a direction along the plate. The total hydrodynamic reaction, the lifting force of Joukowsky, $\overline{R}$, is the vector sum of forces $\overline{P}$ and $\overline{S}$:

(1) See Fig. 14

$$\overline{R} = \overline{P} + \overline{S}$$

The analogy of the flow in the space under the place in the case of planing at small angles of attack, and in the case of the plate fully immersed in a fluid, is valid from the trailing edge to close proximity of the leading edge. Analogous also are pressure distributions in this part of both flows.

The flow is different only in the region of close proximity to the leading edge where the spray jet directed forward occurs along the plate (Fig. 138,b).(1)

From the above reasoning, the results of the study of flow about a plate fully immersed in a fluid can be used for the study of flow under the planing surface if the flow about the leading edge (where velocities grow to infinity) is replaced by streamline flow reproducing the spray jet. Such a replacement at small angles of trim will cause but an immaterial change in the area of the noraml pressure plot diagram at the lower edge of the plate. Taking into account the fact that the flow in planing occupies only the lower part of the space, it can be expected that the resultant of the normal force $\overline{R}$ at the planing surface is equal to:

$$\overline{R} = \overline{P}/2.$$

The validity of this relationship was already noted earlier.

Developing the analogy, we can suppose that the reaction of the spray jet is directed in the opposite sense to the force of suction $\overline{S}$, and in magnitude is equal to $R_b = S/2$. Making use of formula (136) for the spray resistance in the case of planing on the surface of a

(1) See Fig. 14

gravity-less fluid

$$R_b = \delta \rho v^2 \,(1+\cos\alpha),$$

and letting $\cos\alpha = 1$ for small angles, α and $R_b = S/2$, we can compute the thickness of the spray jet:

$$\delta = \frac{S}{4\pi V^2}$$

where S = suction force of the wing and is given as:

$$S = 2\pi\rho\, a\, V^2\alpha^2$$

The validity of the above analogy is confirmed experimentally at large Froude numbers up to values of the angle, α, from 7 to 10 degrees.

In the case of flat plate planing at an arbitrary angle of trim, the resultant of hydrodynamic forces, R, can be calculated by formula (137)

$$R = \rho V^2 \delta \,\mathrm{ctg}\,\frac{\alpha}{2}$$

The curve $K = f(\alpha)$, showing the ratio of the magnitude of force R, calculated by formula (137) to the magnitudes calculated by formula (141), (i.e. on assumption of small angles, α), is plotted on Fig. 139.(1) Fig. 139 shows that with increase of the angle, α, the magnitude of the resultant hydrodynamic pressure, computed by non-linear theory, becomes smaller than that computed by linear theory, i.e. the analogy between the planing surface and a wing is disturbed.

The theory of planing permits one to appraise the effect of shallow water and of limited channel width on the hydrodynamic characteristics of planing surfaces.

(1) See Fig. 14

The detailed investigation of the effects of shallow water on planing upon a gravity-less fluid at various angles of trim was made by U. S. Chaplygin.

As a result of these investigations it is established that, in planing on shallow water at small angles of attack, the analogy with the wing moving between parallel walls is observed. Theoretical calculations show that hydrodynamic characteristics in motion on shallow water depend on the ratio ℓ:h, and the angle α, where h is the water depth.

With increase of the ratio ℓ:h, i.e. with a decrease of water depth, the lifting force at constant velocity increases.

On Fig. 140,(1) curves are given permitting one to estimate the increase of the lifting forces caused by shallowness of water at various values of the parameter ℓ:h and angles of trim, α.

Taking into consideration the effect of channel walls on planing without consideration of gravity indicates that, at the ratio of channel width to the width of the plate b:B $<$ 7, hydrodynamic forces acting on the plate increase; at b:B $>$ 7 the effect of walls leads to a small (less than 2%) reduction of forces as compared to motion on the surface of unbounded fluid.

(1) See Fig. 14

TABLE I

Tabulation of Coefficients for Computation of C_L
Using $\mathring{m}$ Based on Geometric Angle of Trim, τ

$A = 0.4\tau^2 \qquad B = 4\sin\tau + \frac{\pi}{2\lambda}$

1	2	3	4	5	6	$\lambda = 0.2$		$\lambda = 0.4$		$\lambda = 0.6$		$\lambda = 0.8$	
$\tau°$	τ_{rad}	τ^2	$.4\tau^2 = A$	$\sin\tau$	$4\sin\tau$	$\pi/2\lambda$	B	$\pi/2\lambda$	B	$\pi/2\lambda$	B	$\pi/2\lambda$	B
2	.0349	.001218	.000487	.0349	.1396	7.854	7.9936	3.927	4.0666	2.618	2.7576	1.9635	2.1031
4	.0698	.004872	.001949	.0698	.2792		8.1332		4.2062		2.8972		2.2427
6	.1047	.010962	.004385	.1045	.4180		8.2720		4.3450		3.0360		2.3815
9	.1571	.02468	.009872	.1564	.6256		8.4796		4.5526		3.2436		2.5891
12	.2094	.04385	.017540	.2079	.8316		8.6856		4.7586		3.4496		2.7951
18	.3142	.09872	.039488	.3090	1.2360		9.0900		5.1630		3.8540		3.1995
24	.4189	.1755	.070200	.4067	1.6268		9.4808		5.5380		4.2448		3.5903
30	.5236	.2742	.10968	.5000	2.0000		9.8540		5.9270		4.6180		3.9635

$\lambda = 1.0$		$\lambda = 2.0$		$\lambda = 4.0$		$\lambda = 6.0$		$\lambda = 8.0$		$\lambda = 10.0$	
$\pi/2\lambda$	B	$\pi/2\lambda$	B	$\pi/2\lambda$	B	$\pi/2\lambda$	B	$\pi/2\lambda$	B	$\pi/2\lambda$	B
1.5708	1.7104	.7854	.9250	.3927	.5323	.2618	.4014	.19635	.33595	.1571	.2967
	1.8500		1.0646		.6719		.5410		.47555		.4363
	1.9888		1.2034		.8107		.6798		.61435		.5751
	2.1964		1.4110		1.0183		.8874		.82195		.7827
	2.4024		1.6170		1.2243		1.0934		1.02795		.9887
	2.8068		2.0214		1.6287		1.4978		1.43235		1.3931
	3.1976		2.4122		2.0195		1.8886		1.82315		1.7839
	3.5708		2.7854		2.3927		2.2618		2.19635		2.1571

TABLE II

Computation of C_L Using $\mathring{m}$ Based on Geometric Angle of Trim, τ

$$C_L = \frac{B(\tau + 2/\pi) + 2 - A}{2} - \sqrt{\left[\frac{B(\tau + 2/\pi) + 2 - A}{2}\right]^2 + 2(A - B\tau)}$$

1	2	3	4	5	6	7
λ	$\tau°$	$\frac{B(\tau+2/\pi)+2-A}{2}$	$(3)^2$	$2(A-B\tau)$	$\sqrt{(3)+(5)}$	C_L
0.2	2	3.683	13.564	-.557	3.606	.077
	4	3.871	14.985	-1.131	3.722	.149
	6	4.064	16.516	-1.723	3.846	.218
	9	4.360	19.010	-2.644	4.045	.315
	12	4.665	21.762	-3.602	4.261	.404
	18	5.301	28.101	-5.633	4.743	.558
	24	5.968	35.617	-7.803	5.274	.694
	30	6.661	44.369	-10.100	5.853	.808
0.4	2	2.365	5.593	-.283	2.304	.061
	4	2.484	6.170	-.583	2.363	.121
	6	2.608	6.802	-.901	2.429	.179
	9	2.801	7.846	-1.430	2.537	.264
	12	3.004	9.024	-1.958	2.658	.346
	18	3.434	11.792	-3.165	2.937	.497
	24	3.887	15.109	-4.500	3.256	.631
	30	4.383	19.210	-5.988	3.635	.748
0.6	2	1.925	3.706	-.191	1.875	.050
	4	2.022	4.088	-.400	1.920	.102
	6	2.123	4.507	-.627	1.970	.153
	9	2.282	5.208	-.999	2.052	.230
	12	2.450	6.003	-1.410	3.142	.308
	18	2.812	7.907	-2.343	2.359	.453
	24	3.210	10.304	-3.416	2.624	.586
	30	3.624	13.133	-4.617	2.918	.706
0.8	2	1.705	2.907	-.141	1.662	.043
	4	1.791	3.208	-.309	1.703	.088
	6	1.880	3.534	-.490	1.745	.135
	9	2.022	4.088	-.793	1.815	.207
	12	2.173	4.722	-1.135	1.893	.280
	18	2.501	6.255	-1.932	2.079	.422
	24	2.860	8.180	-2.868	2.305	.555
	30	3.244	10.524	-3.931	2.568	.676

TABLE II (Cont'd.)

1	2	3	4	5	6	7
λ	$\tau°$	$\frac{B(\tau+2/\pi)+2-A}{2}$	$③^2$	$2(A-B\tau)$	$\sqrt{③+⑤}$	C_L
1.0	2	1.574	2.477	-.118	1.536	.038
	4	1.652	2.729	-.254	1.573	.079
	6	1.735	3.010	-.407	1.612	.123
	9	1.866	3.482	-.670	1.677	.189
	12	2.007	4.028	-.971	1.748	.259
	18	2.314	5.355	-1.685	1.916	.398
	24	2.652	7.033	-2.539	2.120	.532
	30	3.016	9.096	-3.520	2.361	.655
2.0	2	1.310	1.716	-.064	1.285	.025
	4	1.375	1.891	-.145	1.321	.054
	6	1.444	2.085	-.243	1.357	.087
	9	1.555	2.418	-.423	1.412	.143
	12	1.675	2.806	-.642	1.471	.204
	18	1.941	3.767	-1.191	1.605	.336
	24	2.238	5.009	-1.881	1.768	.470
	30	2.561	6.559	-2.698	1.965	.596
4.0	2	1.178	1.388	-.036	1.163	.015
	4	1.236	1.528	-.090	1.199	.037
	6	1.298	1.685	-.161	1.234	.064
	9	1.399	1.957	-.300	1.287	.112
	12	1.509	2.277	-.478	1.341	.168
	18	1.754	3.077	-.944	1.460	.294
	24	2.031	4.125	-1.552	1.604	.427
	30	2.333	5.443	-2.287	1.776	.557
6.0	2	1.134	1.286	-.027	1.122	.012
	4	1.190	1.416	-.071	1.160	.030
	6	1.250	1.563	-.133	1.196	.054
	9	1.347	1.814	-.259	1.247	.100
	12	1.453	2.111	-.423	1.299	.154
	18	1.692	2.863	-.862	1.414	.278
	24	1.961	3.846	-1.442	1.550	.411
	30	2.257	5.094	-2.150	1.715	.542
8.0	2	1.112	1.236	-.022	1.102	.010
	4	1.167	1.362	-.062	1.140	.027
	6	1.225	1.501	-.120	1.175	.050
	9	1.321	1.745	-.238	1.227	.094
	12	1.426	2.033	-.395	1.280	.146
	18	1.661	2.759	-.821	1.392	.269
	24	1.927	3.713	-1.387	1.525	.402
	30	2.219	4.924	-2.081	1.686	.533

TABLE II (Cont'd.)

1	2	3	4	5	6	7
λ	τ°	$\frac{B(\tau+2/\pi)+2-A}{2}$	$(3)^2$	$2(A-B\tau)$	$\sqrt{(3)+(5)}$	C_L
10	2	1.099	1.208	-.020	1.089	.010
	4	1.153	1.329	-.057	1.128	.025
	6	1.211	1.466	-.111	1.164	.047
	9	1.305	1.703	-.226	1.215	.090
	12	1.409	1.985	-.379	1.267	.142
	18	1.642	2.696	-.796	1.378	.264
	24	1.906	3.633	-1.355	1.509	.397
	30	2.196	4.822	-2.040	1.668	.528

TABLE III

Computation of Lift Coefficient Using a Virtual Mass, $\dot{m}$
Based on Effective Angle of Attack, α_e

$$C_L^3 + \left[\left(2.292 - \frac{1.571}{\lambda}\right)\tau - 2.379 - \frac{1}{\lambda}\right] C_L^2$$

$$\left[\frac{2}{\lambda} + 4 + \left(\frac{6.283}{\lambda} - 4.584\right)\tau\right] C_L - \frac{6.283\,\tau}{\lambda} = 0$$

1	2	3	4	5	6
λ	τ deg	Coeff of C_L^2	Coeff of C_L	Const	Solution
		p	q	r	C_L
1	2	-3.354	6.059	-.219	.036
	4	-3.329	6.119	-.439	.074
	6	-3.304	6.178	-.658	.113
	9	-3.266	6.267	-.987	.166
	12	-3.228	6.356	-1.316	.232
	18	-3.152	6.534	-1.974	.350
	24	-3.077	6.712	-2.631	.482
	30	-3.002	6.889	-3.288	.610
2	2	-2.826	4.950	-.110	.022
	4	-2.774	4.900	-.219	.045
	6	-2.721	4.850	-.329	.070
	9	-2.642	4.774	-.494	.110
	12	-2.563	4.698	-.658	.151
	18	-2.406	4.547	-.987	.250
	24	-2.248	4.397	-1.316	.360
	30	-2.090	4.245	-1.644	.480
4	2	-2.563	4.395	-.055	.012
	4	-2.496	4.290	-.110	.026
	6	-2.430	4.185	-.164	.040
	9	-2.331	4.027	-.247	.064
	12	-2.231	3.870	-.329	.090
	18	-2.032	3.553	-.494	.155
	24	-1.833	3.238	-.658	.237
	30	-1.635	2.923	-.822	.330
6	2	-2.475	4.210	-.037	.009
	4	-2.404	4.086	-.073	.017
	6	-2.333	3.963	-.110	.028
	9	-2.227	3.777	-.164	.044
	12	-2.121	3.592	-.219	.060
	18	-1.908	3.222	-.329	.110
	24	-1.696	2.852	-.438	.170
	30	-1.484	2.481	-.548	.240

TABLE III (Cont'd.)

1	2	3	4	5	6
λ	τ deg	Coeff of C_L^2 p	Coeff of C_L q	Const r	Solution C_L
8	2	-2.431	4.118	-.027	.007
	4	-2.358	3.985	-.055	.014
	6	-2.285	3.852	-.082	.021
	9	-2.175	3.656	-.123	.033
	12	-2.065	3.454	-.164	.049
	18	-1.845	3.056	-.247	.085
	24	-1.626	2.659	-.329	.134
	30	-1.407	2.261	-.411	.200
10	2	-2.404	4.062	-.022	.005
	4	-2.330	3.924	-.044	.011
	6	-2.255	3.786	-.066	.018
	9	-2.144	3.579	-.099	.029
	12	-2.032	3.372	-.132	.040
	18	-1.808	2.957	-.197	.069
	24	-1.585	2.543	-.263	.110
	30	-1.362	2.129	-.329	.160

TABLE IV

DATA SHEET

Run No.	Picture No.	Speed ft/sec V	Trim deg τ	Load on Water lbs	Static Wt. of Apparatus lbs	Load Applied to Loading Arm lbs	HEAVE Ref.	HEAVE Run	HEAVE Diff	REMARKS
1	549	27.72	18	10.61	8.28	2.33	0.93	2.10	1.17	Apparatus clear of spray
2	550	"		10.61		2.33		2.10	1.17	Apparatus clear of spray (some oscillation in speed)
3	551	27.78		18.05		9.77		3.70	2.77	
4	552	"		18.05		9.77		3.70	2.77	
5	553	27.72		21.84		13.56		4.63	3.70	
6	554	"		21.84		13.56		4.60	3.67	
7	555	27.78		24.71		16.43		5.10	4.23	Just off heave stop--at 5.20? No! See next run
8	556	"		24.71		16.43		5.30	4.37	Reset heave stop at 5.40--Just off stop? Yes, read 5.2 with stop at 5.6
9	557	27.72	24	14.81	8.28	6.53	0.00	1.80	1.80	Apparatus clear of spray
10	558	"		14.81		6.53		1.78	1.78	
11	559	"		27.54		19.26		4.25	4.25	
12	560	"		27.54		19.26		4.20	4.20	
13	561	27.66		32.76		24.48		5.33	5.33	(Stop set at 5.70)
14	562	27.72		32.76		24.48		5.25	5.25	
15	563	"		19.93		11.65		2.66	2.66	
16	564	"		19.93		11.65		2.65	2.65	
17	565	27.72	30	18.93	8.28	10.65	-0.65	1.23	1.88	Bottom stop 0.80
18	566	27.84		18.93		10.65		1.20	1.85	
19	567	27.72		36.69		28.41		4.25	4.90	
20	568	"		36.69		28.41		4.25	4.90	(Some spray on loading block)
21	569	"		44.10		35.82		5.65	6.30?	On stop? (Some spray on loading block)
22	570	"		40.28		32.00		4.98	5.63	
23	---	27.78		27.73		19.45		2.70	3.35	
24	571	27.90		27.73		19.45		2.65	3.30	

TABLE V

Wave Rise "Correction" Factors for Wetted Length Determinations from Heave Readings

b = 2"

Angle of Trim τ (deg.)	Photo No.	Velocity V (ft/sec.)	Speed Coeff. C_v	Wetted Length/Beam Ratio from Photo λ	Heave (Reading Minus Ref.) h	h/b $\sin\tau$	Wave Rise Factor (λ-h/b $\sin\tau$)
	549	27.72	11.96	2.30	1.17	1.89	.41
	550	27.72	11.96	2.30	1.17	1.89	.41
	551	27.78	11.99	5.07	2.77	4.49	.58
	552	27.78	11.99	5.05	2.77	4.49	.56
18°	553	27.72	11.96	6.55	3.70	6.00	.55
	554	27.72	11.96	6.43	3.67	5.95	.48
	555	27.78	11.99	7.22	4.23	6.85	.37
	556	27.78	11.99	7.44	4.37	7.08	.36
	557	27.72	11.96	2.68	1.80	2.22	.46
	558	27.72	11.96	2.63	1.78	2.19	.44
	559	27.72	11.96	5.87	4.25	5.23	.64
	560	27.72	11.96	5.82	4.20	5.16	.66
24°	561	27.66	11.94	7.25	5.33	6.55	.70
	562	27.72	11.96	7.12	5.25	6.45	.67
	563	27.72	11.96	3.80	2.66	3.27	.43
	564	27.72	11.96	3.80	2.65	3.26	.54
	565	27.72	11.96	2.52	1.88	1.88	.64
	566	27.84	12.02	2.42	1.85	1.85	.57
	567	27.72	11.96	5.72	4.90	4.90	.82
30°	568	27.72	11.96	5.67	4.90	4.90	.77
	569	27.72	11.96	7.03	6.30	6.30	.73
	570	27.72	11.96	6.37	5.63	5.63	.74
	571	27.90	12.04	4.00	3.30	3.30	.70

TABLE VI

Reduction of Experimental Data, Correlating C_L and λ

$\frac{\rho}{2} = .97 \frac{\text{slugs}}{\text{ft.}^3}$ $b^2 = .02777 \text{ ft.}^2$ $q = \frac{1}{2}\rho V^2 \frac{\text{slug ft.}}{\text{sec.}^2}$

$$C_L = \frac{L}{q\, b^2\, \lambda}$$

Pict.	V	C_v	q	λ	λb^2	$q\lambda b^2$	L	C_L
549	27.72	11.96	745.35	2.30	.06387	47.6055	10.61	.223
550	27.72	11.96	745.35	2.30	.06387	47.6055	10.61	.223
551	27.78	11.99	748.58	5.07	.1408	105.40	18.05	.171
552	27.78	11.99	748.58	5.05	.1402	104.95	18.05	.172
553	27.72	11.96	745.35	6.55	.1819	135.58	21.84	.161
554	27.72	11.96	745.35	6.43	.1786	133.12	21.84	.164
555	27.78	11.99	748.58	7.22	.2005	150.09	24.71	.165
556	27.78	11.99	748.58	7.44	.2066	154.66	24.71	.160
557	27.72	11.96	745.35	2.68	.07442	55.47	14.81	.267
558	27.72	11.96	745.35	2.63	.07304	54.44	14.81	.272
559	27.72	11.96	745.35	5.87	.1630	121.49	27.54	.227
560	27.72	11.96	745.35	5.82	.1616	120.45	27.54	.229
561	27.66	11.94	742.13	7.25	.2013	149.39	32.76	.219
562	27.72	11.96	745.35	7.12	.1977	147.36	32.76	.222
563	27.72	11.96	745.35	3.80	.1055	78.63	19.93	.253
564	27.72	11.96	745.35	3.80	.1055	78.63	19.93	.253
565	27.72	11.96	745.35	2.52	.06998	52.16	18.93	.363
566	27.84	12.02	751.82	2.42	.06720	50.52	18.93	.375
567	27.72	11.96	745.35	5.72	.1588	118.36	36.69	.310
568	27.72	11.96	745.35	5.67	.1575	117.39	36.69	.313
569	27.72	11.96	745.35	7.03	.1952	145.49	44.10	.303
570	27.72	11.96	745.35	6.37	.1769	131.85	40.28	.305
571	27.90	12.04	755.06	4.00	.1111	83.88	27.73	.331

TABLE VII

Tabulation of Computed and Experimental Results for the Gravity Independent Lift Coefficient

1	2	3	4	5	6	7	8
				Definition of $\dot{m}$ Based on τ		Definition of $\dot{m}$ Based on α_e	
λ	τ	C_V	$C_{L\,Exp}$	$C_{L\,Comp}$	$\frac{C_{L\,Comp}}{C_{L\,Exp}}$	$C_{L\,Comp}$	$\frac{C_{L\,Comp}}{C_{L\,Exp}}$
.30	2^{o}	21.44	.031	.067	2.16	.072	2.32
.40		18.51	.031	.060	1.935	.065	2.10
.45		24.61	.031	.058	1.87	.063	2.03
.62		20.53	.033	.049	1.485	.052	1.58
.68		20.74	.029	.046	1.585	.049	1.69
.70		24.92	.029	.045	1.55	.048	1.65
.87		14.55	.023	.041	1.78	.041	1.78
.87		22.88	.028	.041	1.46	.041	1.46
1.17		20.04	.027	.035	1.30	.033	1.22
1.57		25.01	.022	.029	1.32	.027	1.23
2.54		13.37	.019	.022	1.16	.020	1.05
3.00		13.66	.015	.020	1.33	.018	1.20
3.00		13.72	.015	.020	1.33	.018	1.20
3.00		16.99	.015	.020	1.33	.018	1.20
3.00		21.87	.015	.020	1.33	.018	1.20
4.79		12.20	.012	.015	1.25	.012	1.00
6.50		25.01	.009	.012	1.33	.008	.89
6.50		18.64	.010	.012	1.20	.008	.80
7.79		13.39	.009	.010	1.11	.005	.555
8.12		23.39	.009	.010	1.11	.005	.555
8.27		12.78	.009	.010	1.11	.005	.555
.25	4^{o}	14.40	.082	.140	1.71	.150	1.83
.35		19.98	.091	.125	1.37	.135	1.48
.38		16.99	.117	.123	1.05	.133	1.14
.38		24.86	.091	.123	1.35	.133	1.46
.50		13.57	.092	.110	1.20	.120	1.31
.54		13.68	.084	.108	1.29	.115	1.37
.62		21.66	.073	.100	1.37	.105	1.44
.85		24.92	.073	.085	1.16	.088	1.20
1.45		21.87	.055	.063	1.14	.057	1.04
1.45		12.81	.054	.063	1.17	.057	1.06
1.50		16.26	.054	.062	1.15	.056	1.04
1.52		16.23	.053	.061	1.15	.055	1.04
1.64		16.37	.048	.059	1.23	.053	1.10
1.66		12.86	.049	.059	1.20	.052	1.06
2.20		24.80	.041	.051	1.24	.042	1.02
3.66		10.97	.029	.039	1.34	.029	1.00
4.07		24.77	.029	.036	1.24	.026	.895
4.54		13.48	.026	.034	1.31	.024	.925
4.63		20.95	.027	.034	1.26	.023	.854
4.66		18.13	.025	.033	1.32	.023	.920
4.82		17.51	.026	.033	1.27	.022	.846
5.14		22.97	.027	.032	1.18	.021	.778
5.54		17.57	.022	.031	1.41	.020	.910
7.16		12.00	.021	.029	1.38	.020	.955
8.54		15.46	.019	.026	1.37	.012	.630

TABLE VII(Cont'd.)

1	2	3	4	5	6	7	8
				Definition of $\mathring{m}$ Based on τ		Definition of $\mathring{m}$ Based on α_e	
λ	τ	C_V	$C_{L\ Exp}$	$C_{L\ Comp}$	$\frac{C_{L\ Comp}}{C_{L\ Exp}}$	$C_{L\ Comp}$	$\frac{C_{L\ Comp}}{C_{L\ Exp}}$
.22	6°	19.89	.147	.207	1.41	.208	1.42
.25		24.77	.139	.205	1.47	.205	1.48
.30		16.68	.153	.194	1.27	.195	1.27
.38		24.92	.163	.181	1.11	.184	1.13
.55		12.69	.143	.158	1.10	.156	1.09
.55		16.32	.145	.158	1.09	.156	1.08
.65		21.90	.123	.150	1.22	.146	1.19
.66		16.27	.122	.149	1.22	.145	1.19
.67		25.10	.131	.148	1.13	.144	1.10
1.32		12.96	.096	.107	1.12	.098	1.02
1.40		24.46	.086	.105	1.22	.094	1.09
1.42		24.10	.088	.104	1.18	.093	1.06
1.42		17.60	.087	.104	1.20	.093	1.07
1.52		20.86	.084	.100	1.19	.090	1.07
1.66		17.37	.076	.095	1.25	.085	1.12
3.00		17.60	.060	.073	1.22	.053	.884
3.05		10.83	.059	.072	1.22	.052	.880
3.22		24.16	.057	.070	1.23	.050	.88
3.32		14.55	.055	.069	1.25	.049	.89
3.35		19.86	.055	.069	1.25	.048	.87
3.41		17.71	.052	.068	1.31	.047	.90
3.79		10.72	.049	.065	1.33	.043	.88
5.20		24.46	.045	.056	1.24	.031	.69
5.57		20.74	.044	.055	1.25	.030	.67
5.62		17.08	.044	.055	1.25	.029	.66
5.62		12.41	.044	.055	1.25	.029	.66
5.75		15.01	.043	.054	1.26	.028	.65
6.29		17.81	.039	.053	1.36	.025	.64
7.29		19.90	.037	.051	1.38	.021	.57
7.66		16.27	.036	.051	1.42	.020	.555
7.79		14.13	.036	.050	1.39	.020	.555
.91	9°	15.70	.171	.197	1.15	.180	1.05
.91		11.83	.167	.197	1.18	.180	1.08
1.86		18.28	.117	.146	1.25	.117	1.00
3.04		11.80	.091	.121	1.33	.081	.89
3.10		14.10	.090	.120	1.33	.080	.89
3.66		15.40	.084	.114	1.36	.069	.82
5.41		13.78	.070	.104	1.49	.048	.69
5.41		11.98	.071	.104	1.47	.048	.68
7.16		10.82	.066	.096	1.45	.037	.56
7.29		12.30	.066	.096	1.45	.036	.55
.08	12°	24.98	.256	.455	1.78	.460	1.80
.10		20.04	.318	.445	1.40	.445	1.40
.12		16.96	.371	.435	1.17	.435	1.17
.12		24.95	.285	.435	1.53	.435	1.53
.15		21.59	.305	.425	1.39	.425	1.39

TABLE VII (Cont'd.)

1	2	3	4	5	6	7	8
				Definition of $\mathring{m}$ Based on τ		Definition of $\mathring{m}$ Based on α_e	
λ	τ	C_V	C_L Exp	C_L Comp	$\frac{C_L \text{ Comp}}{C_L \text{ Exp}}$	C_L Comp	$\frac{C_L \text{ Comp}}{C_L \text{ Exp}}$
.20	12°	25.16	.302	.400	1.33	.410	1.36
.20		12.75	.393	.400	1.02	.410	1.04
.25		16.23	.324	.385	1.19	.390	1.20
.28		21.59	.294	.380	1.29	.385	1.31
.30		25.25	.291	.370	1.27	.375	1.29
.31		24.98	.198	.367	1.85	.372	1.88
.40		13.79	.280	.345	1.23	.345	1.23
.40		17.32	.318	.345	1.08	.345	1.08
.45		21.14	.276	.333	1.21	.335	1.21
.48		24.40	.254	.328	1.29	.330	1.30
.53		12.26	.268	.319	1.19	.315	1.18
.54		12.22	.264	.318	1.20	.312	1.18
.70		17.54	.257	.295	1.15	.275	1.07
.75		24.40	.238	.288	1.21	.268	1.12
.75		20.07	.240	.288	1.20	.268	1.11
.77		10.80	.236	.285	1.21	.266	1.13
1.15		24.49	.204	.248	1.22	.214	1.05
1.17		20.89	.209	.247	1.18	.213	1.01
1.20		14.95	.206	.243	1.18	.210	1.02
1.22		12.38	.204	.242	1.19	.208	1.02
1.25		12.50	.195	.240	1.23	.205	1.05
1.80		24.28	.164	.210	1.28	.164	1.00
2.00		23.27	.161	.204	1.27	.152	.94
2.05		14.94	.157	.202	1.29	.150	.96
2.07		21.01	.154	.201	1.31	.149	.97
2.62		16.78	.143	.187	1.31	.125	.87
2.66		12.22	.140	.185	1.32	.125	.89
2.90		21.01	.136	.181	1.33	.116	.85
2.92		11.74	.138	.180	1.31	.115	.83
2.97		20.74	.136	.180	1.32	.114	.84
3.00		16.23	.134	.179	1.34	.113	.84
3.07		16.13	.132	.178	1.35	.112	.85
4.05		16.78	.123	.167	1.36	.088	.72
4.07		10.52	.122	.167	1.37	.087	.71
4.12		18.67	.121	.166	1.37	.086	.71
4.20		14.55	.120	.165	1.37	.085	.71
4.25		12.02	.118	.165	1.40	.085	.72
.12	18°	25.10	.508	.585	1.15	.580	1.14
.18		12.69	.441	.560	1.27	.560	1.27
.18		21.75	.450	.560	1.24	.560	1.24
.18		25.50	.473	.560	1.18	.560	1.18
.20		10.13	.622	.550	.885	.550	.88
.25		21.26	.490	.535	1.09	.525	1.07
.26		15.49	.342	.533	1.56	.523	1.53
.28		10.13	.444	.529	1.19	.515	1.16
.28		17.23	.461	.529	1.14	.515	1.11

TABLE VII (Cont'd.)

1	2	3	4	5	6	7	8
				Definition of $\mathring{m}$ Based on τ		Definition of $\mathring{m}$ Based on α_e	
λ	τ	C_V	$C_{L\ Exp}$	$C_{L\ Comp}$	$\frac{C_{L\ Comp}}{C_{L\ Exp}}$	$C_{L\ Comp}$	$\frac{C_{L\ Comp}}{C_{L\ Exp}}$
.28	18°	21.01	.448	.529	1.18	.515	1.15
.28		24.43	.433	.529	1.22	.515	1.19
.35		24.40	.511	.505	.987	.487	.95
.40		17.63	.446	.492	1.10	.470	1.05
.40		10.74	.442	.492	1.11	.470	1.06
.42		10.83	.432	.488	1.13	.465	1.07
.44		19.82	.419	.482	1.15	.460	1.10
.58		15.01	.424	.456	1.08	.426	1.01
.58		24.61	.400	.456	1.14	.425	1.06
.60		20.83	.409	.450	1.10	.420	1.03
.65		12.44	.381	.441	1.16	.416	1.09
.90		23.18	.361	.408	1.13	.368	1.02
.92		10.98	.346	.406	1.17	.364	1.05
.95		14.91	.343	.403	1.17	.361	1.05
1.02		21.01	.312	.395	1.26	.350	1.12
1.35		16.31	.296	.368	1.26	.310	1.05
1.38		20.98	.287	.366	1.27	.307	1.07
1.47		16.20	.276	.362	1.31	.299	1.08
1.50		15.65	.290	.359	1.24	.294	1.01
1.55		12.99	.276	.356	1.29	.289	1.05
1.87		16.78	.266	.343	1.29	.261	.98
1.88		14.61	.265	.343	1.29	.260	.98
1.98		14.70	.249	.339	1.36	.254	1.02
2.02		18.64	.249	.337	1.35	.250	1.00
2.02		16.80	.247	.337	1.36	.250	1.01
2.02		11.90	.253	.337	1.33	.250	.99
2.30		11.96	.223	.328	1.47	.230	1.03
2.30		11.96	.223	.328	1.47	.230	1.03
5.07		11.99	.171	.284	1.66	.127	.74
5.05		11.99	.172	.284	1.65	.128	.74
6.43		11.96	.164	.275	1.68	.104	.63
6.55		11.96	.161	.274	1.70	.102	.63
7.22		11.99	.165	.272	1.65	.094	.57
7.44		11.99	.160	.271	1.69	.091	.57
.22	24°	21.11	.565	.680	1.20	.686	1.21
.22		17.35	.579	.680	1.18	.686	1.19
.24		13.02	.523	.673	1.29	.675	1.29
.25		10.10	.501	.671	1.34	.675	1.35
.32		17.45	.568	.645	1.14	.650	1.16
.32		20.04	.563	.645	1.15	.650	1.15
.32		24.40	.558	.645	1.16	.650	1.17
.38		24.34	.473	.635	1.34	.636	1.35
.38		10.80	.480	.635	1.32	.636	1.33
.44		24.61	.527	.618	1.17	.615	1.17
.45		20.86	.544	.617	1.13	.614	1.13
.49		12.47	.503	.610	1.21	.608	1.21
.50		15.01	.492	.605	1.23	.604	1.23

TABLE VII(Cont'd.)

1	2	3	4	5	6	7	8
				Definition of $\mathring{m}$ Based on τ		Definition of $\mathring{m}$ Based on α_e	
λ	τ	C_V	$C_{L\ Exp}$	$C_{L\ Comp}$	$\frac{C_{L\ Comp}}{C_{L\ Exp}}$	$C_{L\ Comp}$	$\frac{C_{L\ Comp}}{C_{L\ Exp}}$
.55	24°	24.95	.510	.594	1.16	.585	1.15
.55		20.77	.448	.594	1.32	.585	1.30
.55		12.41	.453	.594	1.31	.585	2.31
.65		18.39	.484	.578	1.20	.560	1.16
.70		14.88	.467	.570	1.22	.550	1.08
.70		20.92	.459	.570	1.24	.550	1.20
.70		23.33	.458	.570	1.25	.550	1.20
.94		11.65	.434	.539	1.24	.500	1.15
.95		13.42	.423	.539	1.27	.498	1.18
.98		20.62	.419	.536	1.28	.495	1.18
1.00		16.16	.408	.533	1.31	.487	1.19
1.17		16.59	.437	.517	1.18	.457	1.05
1.22		18.54	.416	.514	1.23	.450	1.08
1.22		11.90	.419	.514	1.23	.450	1.07
1.27			.399	.510	1.28	.443	1.11
2.63		11.96	.272	.452	1.66	.308	1.13
2.68		11.96	.267	.451	1.69	.306	1.15
3.80		11.96	.253	.430	1.70	.245	.97
5.82		11.96	.229	.412	1.80	.175	.77
5.87		11.96	.227	.412	1.81	.174	.77
7.12		11.96	.222	.406	1.83	.148	.67
7.25		11.94	.219	.405	1.85	.146	.67
.11	30°	21.72	.739	.826	1.12	.835	1.13
.11		16.41	.719	.826	1.15	.835	1.16
.11		12.78	.711	.826	1.16	.835	1.17
.12		24.98	.740	.822	1.11	.830	1.12
.16		20.86	.796	.814	1.02	.820	1.03
.16		17.63	.771	.814	1.05	.820	1.06
.18		10.13	.692	.807	1.17	.816	1.18
.27		17.45	.674	.783	1.16	.785	1.16
.27		10.89	.665	.783	1.18	.785	1.18
.31		20.10	.578	.770	1.33	.765	1.32
.40		12.41	.622	.749	1.20	.749	1.20
.40		14.91	.623	.749	1.20	.749	1.20
.54		14.98	.598	.718	1.20	.711	1.19
.73		13.24	.566	.686	1.21	.668	1.18
.98		11.99	.514	.658	1.28	.622	1.21
.98		14.49	.518	.658	1.27	.622	1.20
2.42		12.02	.375	.583	1.55	.443	1.18
2.52		11.96	.363	.581	1.60	.435	1.20
4.00		12.04	.331	.557	1.68	.330	1.06
5.67		11.96	.313	.544	1.73	.253	.81
5.72		11.96	.310	.543	1.75	.252	.81
6.37		11.96	.305	.540	1.77	.234	.77
7.03		11.96	.303	.537	1.77	.217	.72

TABLE VIII

Empirical Correction to C_L Computed from the Cubic Equation

Definition of $\mathring{m}$ Based on α_e

$$\frac{C_L \text{ computed}}{\eta} = C_L \text{ corrected}$$

$$\eta_2 = 1.359\text{-tanh } \frac{1+\lambda}{8} + \frac{\Delta\tau}{1.58} \text{ tanh } \lambda^2$$

$$\eta_1 = 1.359\text{-tanh } \left(\frac{1+\lambda}{8}\right)$$

τ^o	λ	1	2	3	4	5	6	7	8	9	10	0
2	C_L computed	.036	.022	.016	.013	.010	.007	.006	.0055	.005	.005	.105
	C_L corrected	.032	.022	.018	.016	.014	.011	.010	.010	.010	.010	.085
4		.075	.045	.033	.026	.021	.017	.015	.013	.011	.010	.197
		.067	.045	.037	.032	.029	.026	.025	.024	.022	.021	.160
6		.113	.071	.050	.040	.033	.026	.024	.022	.0205	.019	.285
		.101	.071	.056	.050	.046	.040	.040	.040	.040	.040	.231
9		.170	.111	.082	.064	.051	.044	.038	.034	.032	.030	.392
		.153	.111	.091	.080	.071	.067	.064	.062	.062	.062	.318
12		.230	.152	.114	.090	.074	.062	.055	.049	.044	.040	.490
		.206	.152	.127	.112	.102	.095	.092	.089	.086	.083	.397
18		.353	.250	.192	.155	.130	.110	.096	.085	.077	.070	.655
		.317	.250	.214	.193	.180	.168	.161	.155	.151	.146	.530
24		.487	.358	.285	.235	.198	.170	.150	.134	.120		.798
		.419	.336	.296	.271	.252	.237	.227	.209	.209		.647
30		.616	.482	.398	.330	.278	.244	.218	.196	.178		.856
		.511	.425	.387	.352	.324	.310	.300	.288	.277		.694

TABLE IX

Values of the Lift Coefficient for Low Aspect Ratio Airfoils

$$C_L = \frac{2\pi\alpha}{1 + \frac{2\lambda\pi}{\pi + 4\lambda \sin}}$$

(C_L found from the momentum equation with $\mathring{m}$ based on α)

$\lambda = 1$		$\lambda = 2$		$\lambda = 2.86$		$\lambda = 7.46$	
α^{o}	C_L	α^{o}	C_L	α^{o}	C_L	α^{o}	C_L
0	0	0	0	0	0	0	0
10	.416	10	.291	10	.244	10	.165
20	.917	20	.699	20	.619	20	.486
30	1.482	30	1.193	30	1.087	30	.915

$$C_L = -\left[\frac{\pi^2}{2}\left(\frac{1}{2\lambda} + 1\right) - \pi\alpha\right] + \sqrt{\left[\frac{\pi^2}{2}\left(\frac{1}{2\lambda} + 1\right) - \pi\alpha\right]^2 + \frac{\pi^3\alpha}{\lambda}}$$

(C_L found from the momentum equation with $\mathring{m}$ based on α_e)

$\lambda = 1$		$\lambda = 2$		$\lambda = 2.86$		$\lambda = 7.46$	
α^{o}	C_L	α^{o}	C_L	α^{o}	C_L	α^{o}	C_L
0	0	0	0	0	0	0	0
10	.384	10	.238	10	.178	10	.076
20	.807	20	.508	20	.388	10	.171
30	1.271	30	.824	30	.637	30	.290

Schematic for Virtual Mass Definitions

Fig. 1

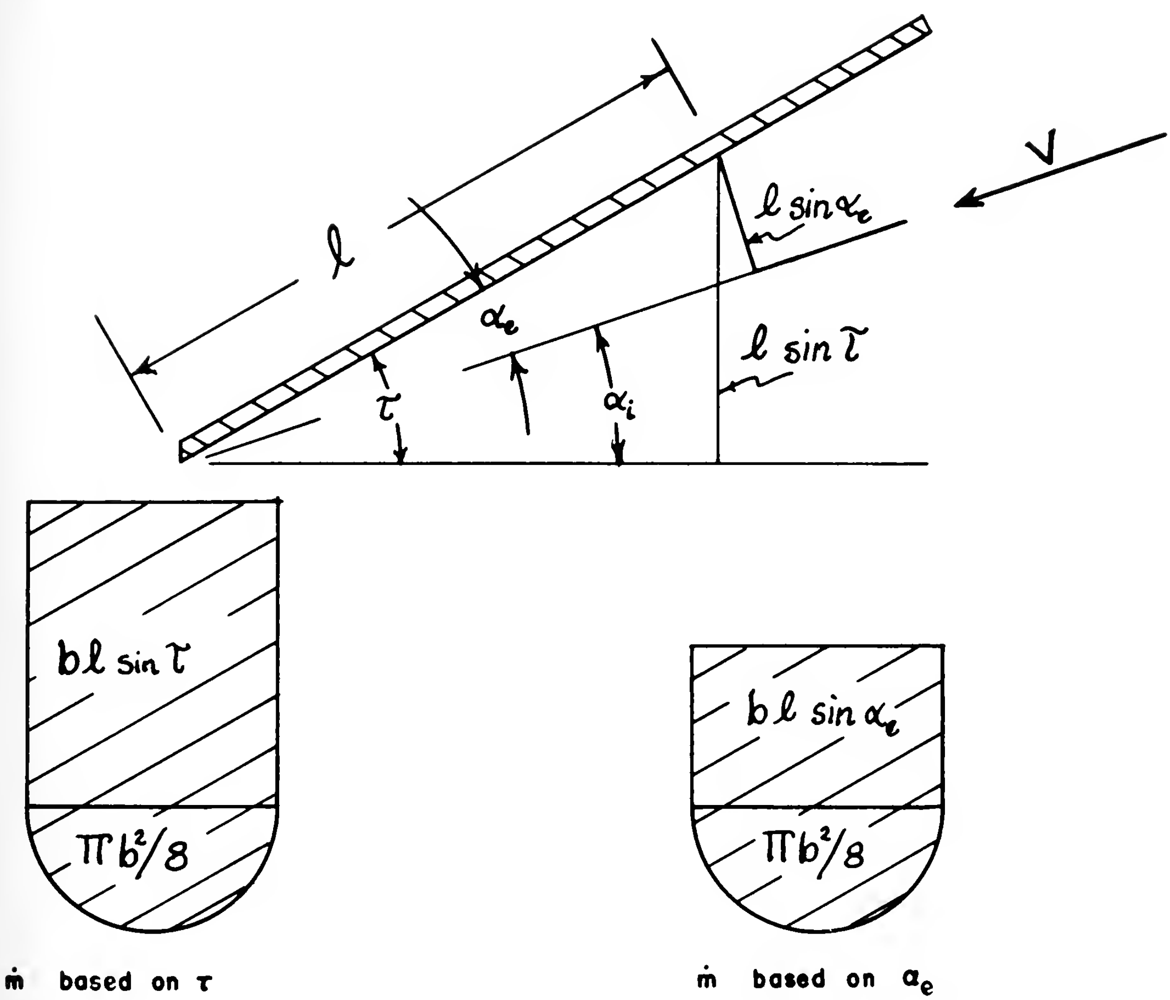

Schematic for Spray Thickness, Stagnation Point, and Spray Root

Fig. 2

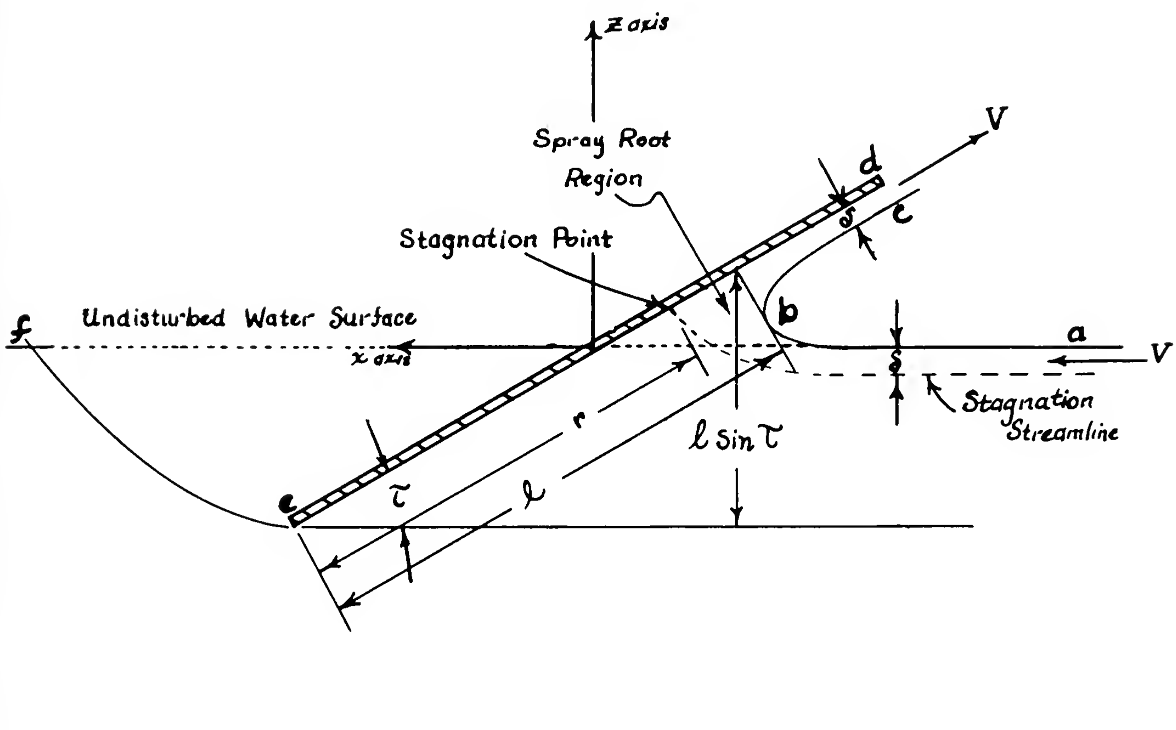

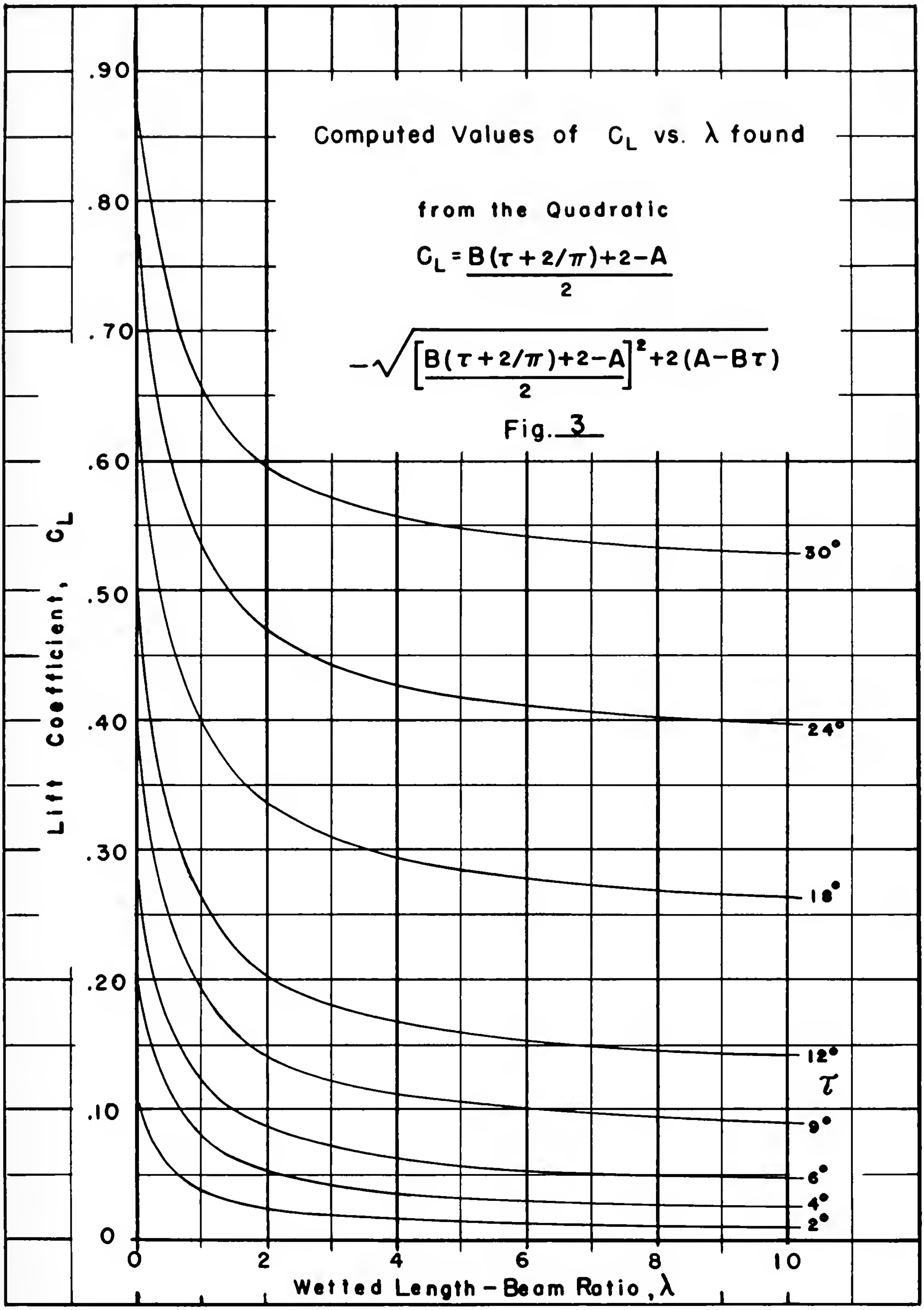

Computed Values of C_L vs. λ found
from the Quadratic
$$C_L = \frac{B(\tau + 2/\pi) + 2 - A}{2} - \sqrt{\left[\frac{B(\tau + 2/\pi) + 2 - A}{2}\right]^2 + 2(A - B\tau)}$$
Fig. 3
Lift Coefficient, C_L
.90
.80
.70
.60
.50
.40
.30
.20
.10
0
0
2
4
6
8
10
Wetted Length – Beam Ratio, λ
30°
24°
18°
12°
τ
9°
6°
4°
2°

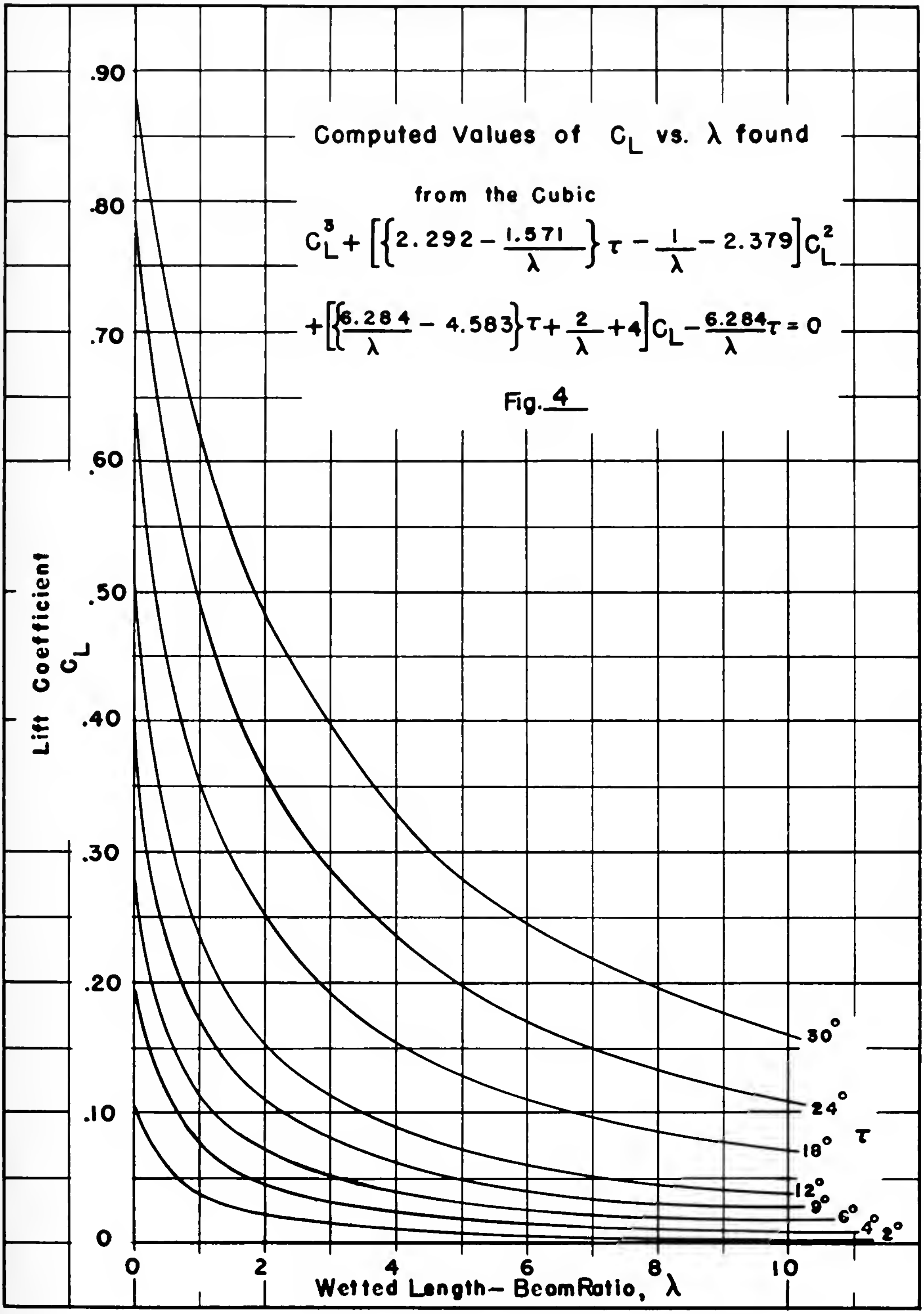

Computed Values of C_L vs. λ found
from the Cubic
$$C_L^3 + \left[\left\{2.292 - \frac{1.571}{\lambda}\right\}\tau - \frac{1}{\lambda} - 2.379\right]C_L^2 + \left[\left\{\frac{6.284}{\lambda} - 4.583\right\}\tau + \frac{2}{\lambda} + 4\right]C_L - \frac{6.284}{\lambda}\tau = 0$$
.90
.80
.70
.60
.50
.40
.30
.20
.10
0
Lift Coefficient C_L
0
2
4
6
8
10
Wetted Length– BeamRatio, λ
30°
24°
18°
12°
9°
6°
4°
2°
τ

Fig. 4

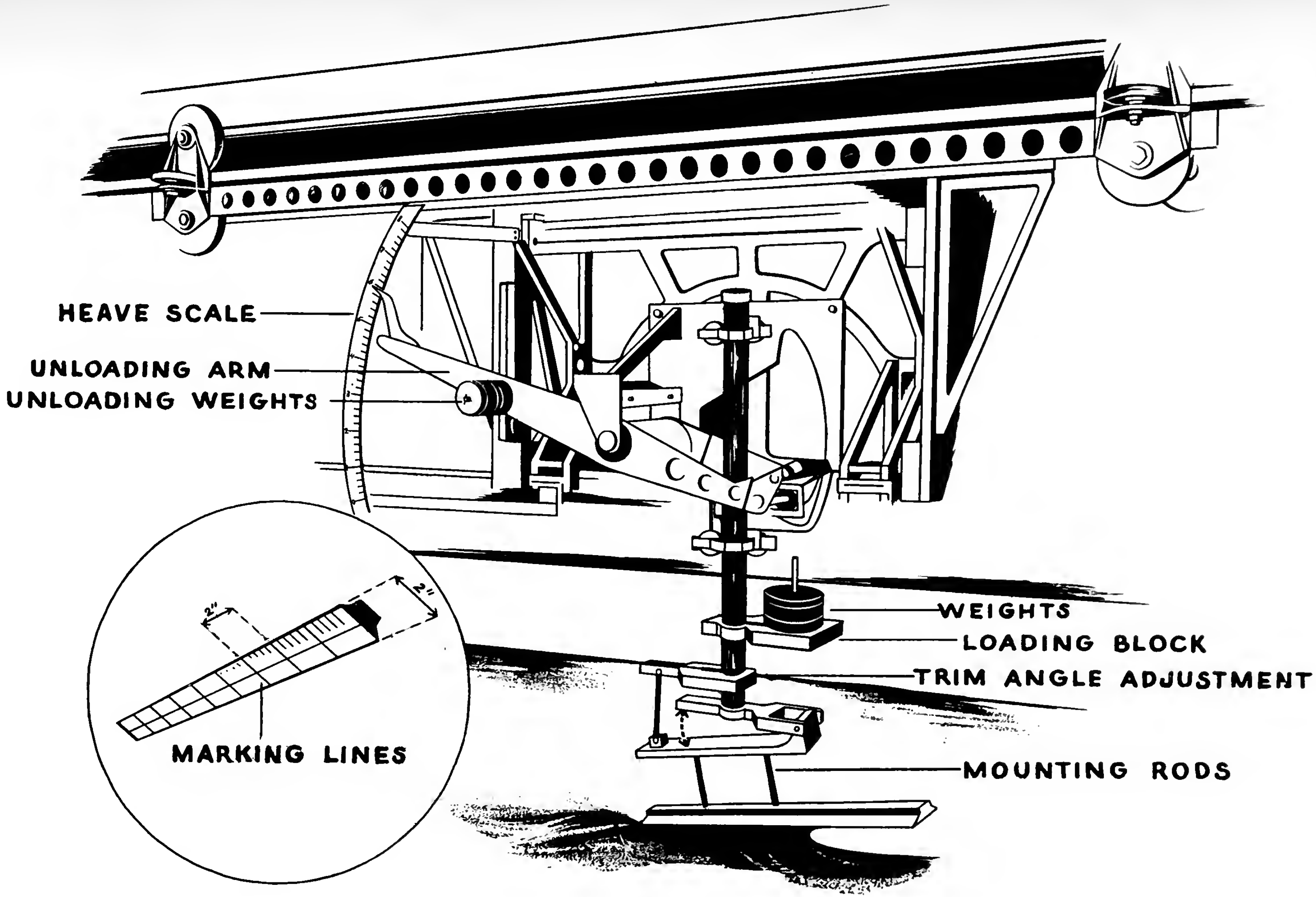

FIG. – 5

Set-Up of Experimental Apparatus

Schematic for Heave Calibration Dimensions

Fig. 6

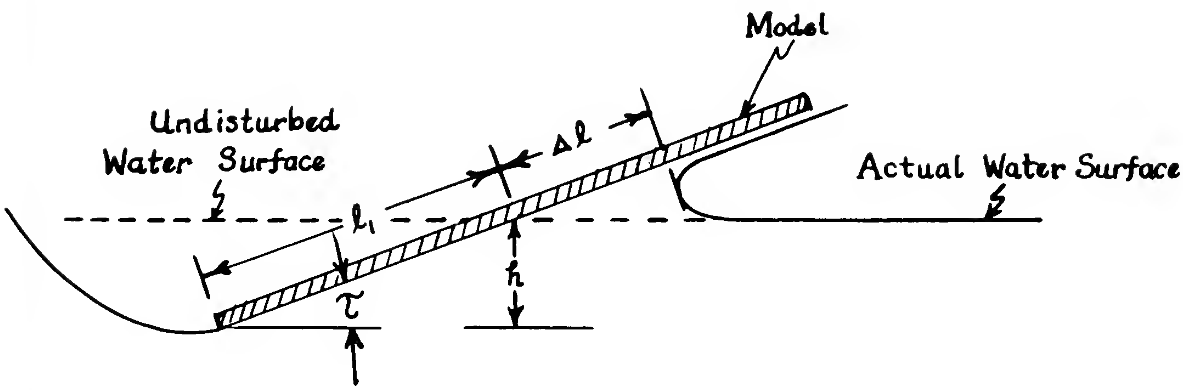

Lift of a Two-Dimensional Flat Plate as a Function of Froude Number

Fig. 7

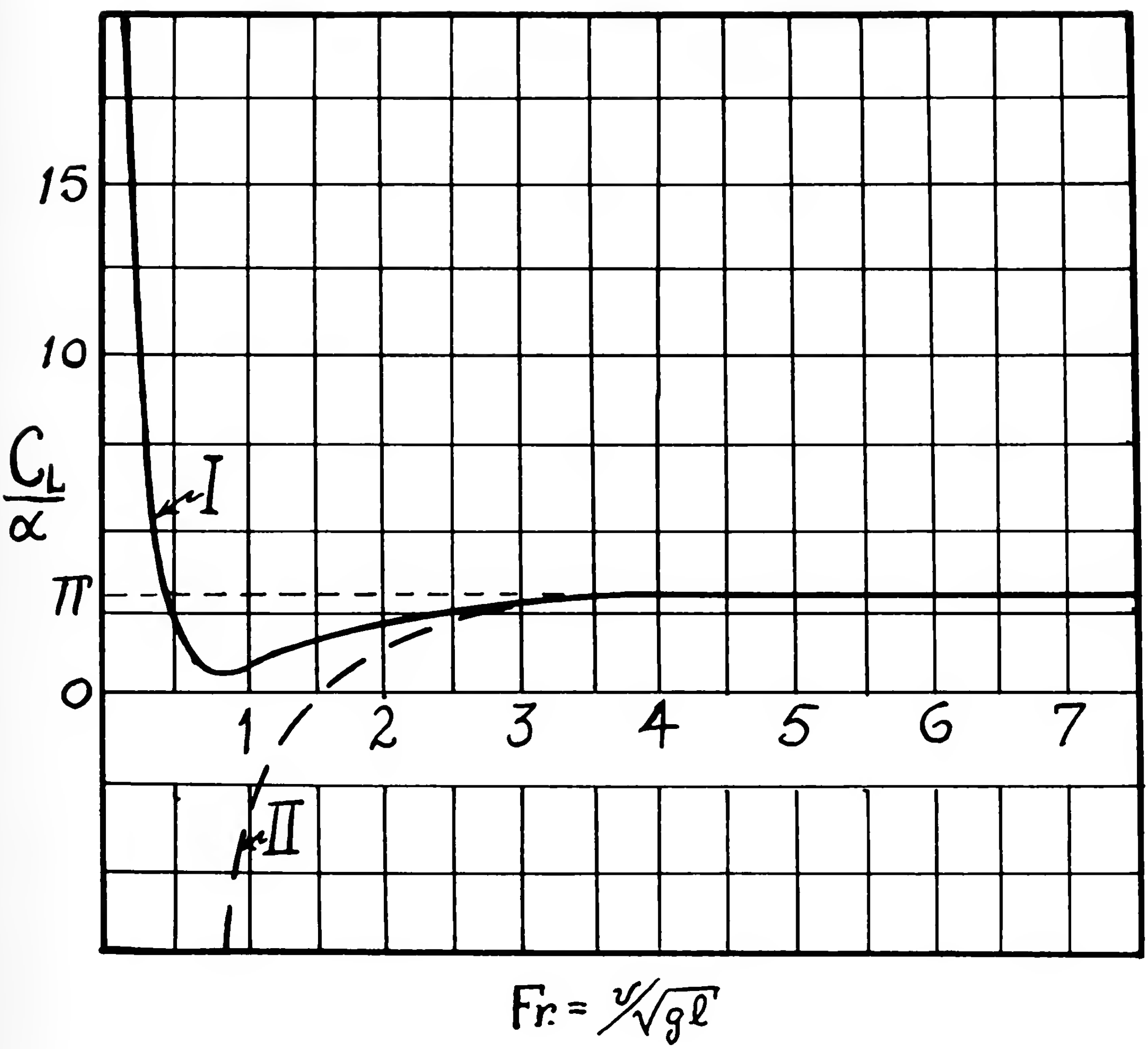

Ratio of $C_{L\,computed}$ to $C_{L\,experimental}$

($\dot{m}$ based on α_e)

Fig. 8

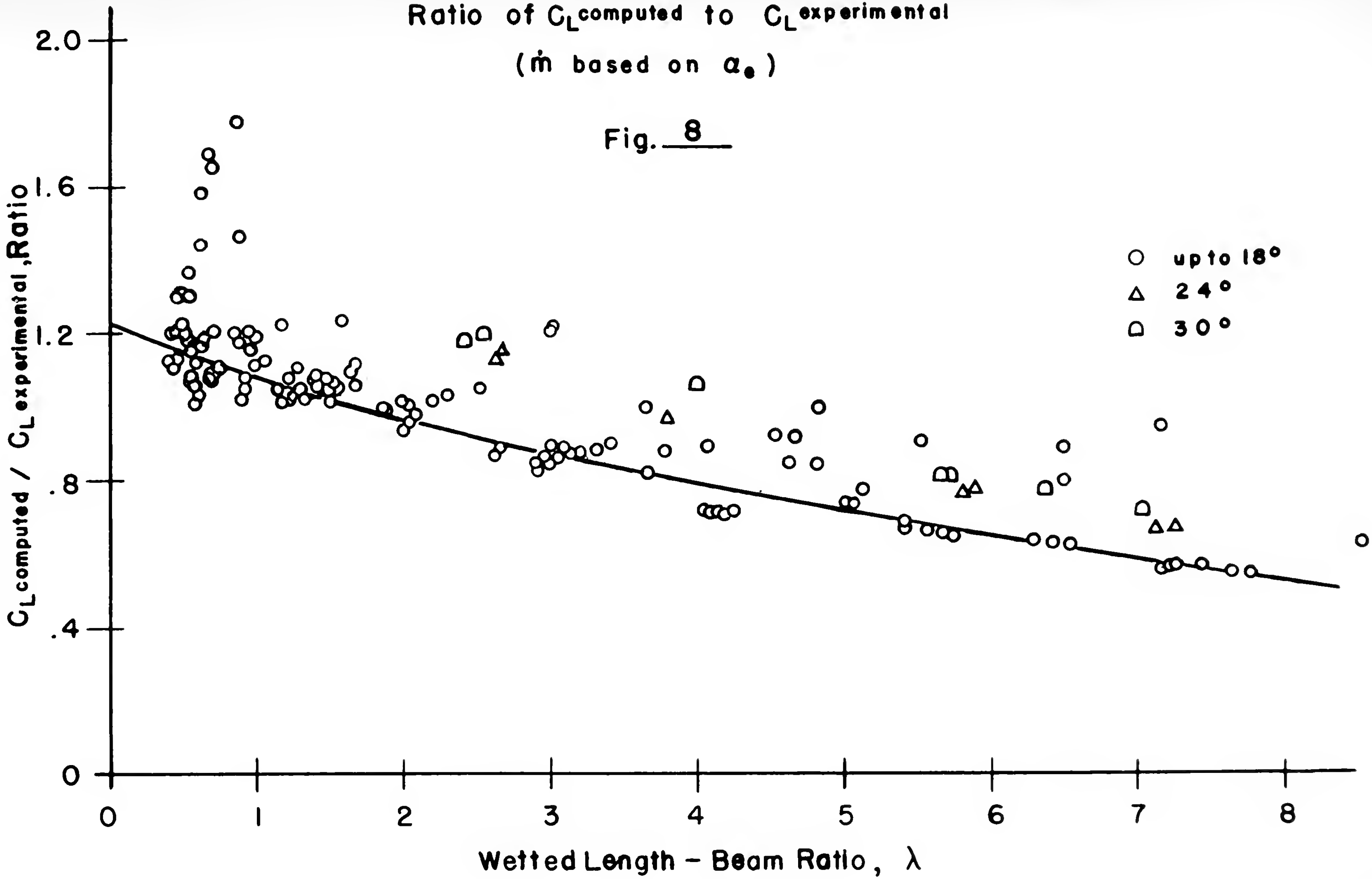

Ratio of $C_{L\,computed}$ to $C_{L\,experimental}$

($\dot{m}$ based on τ)

Fig. 9

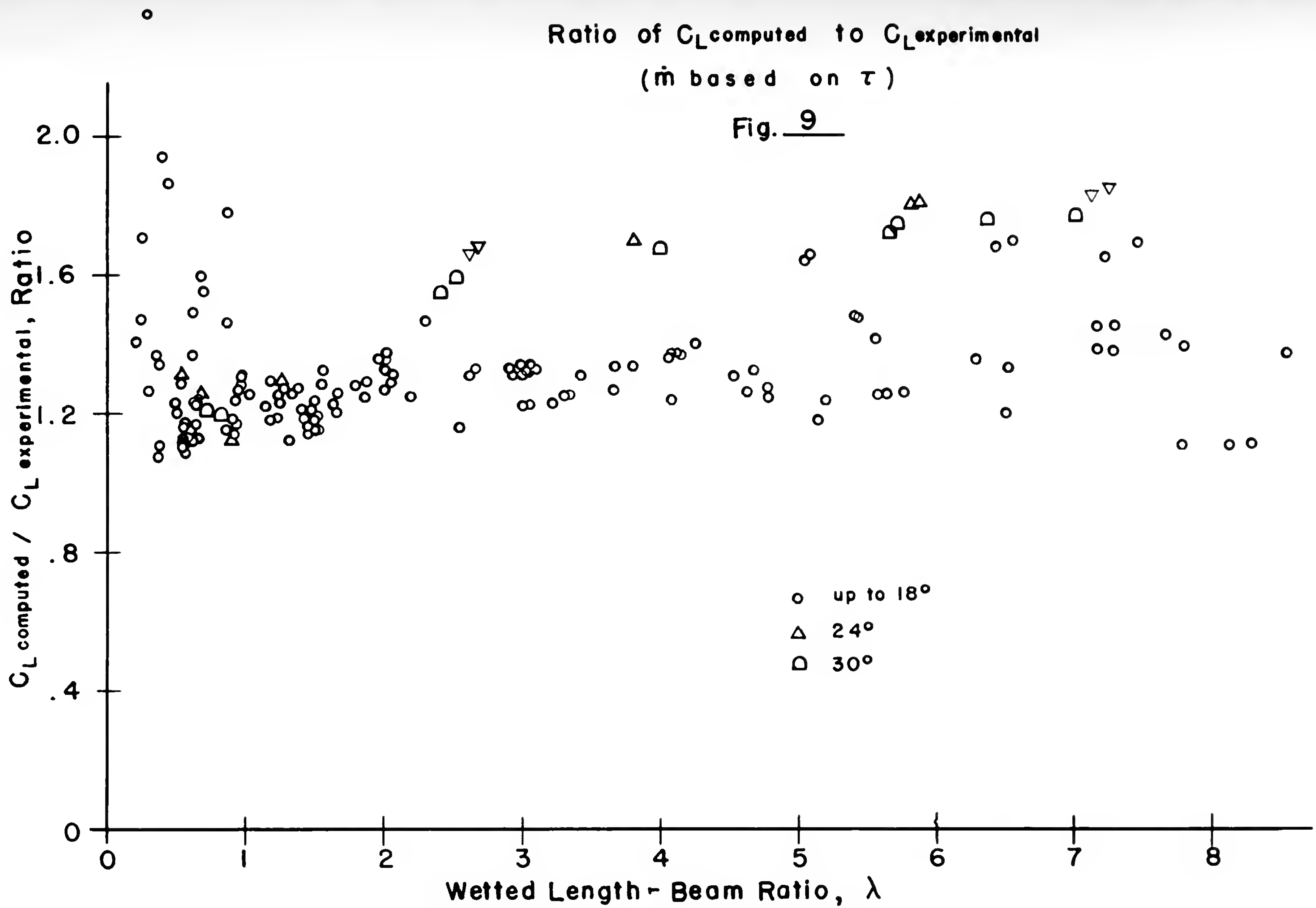

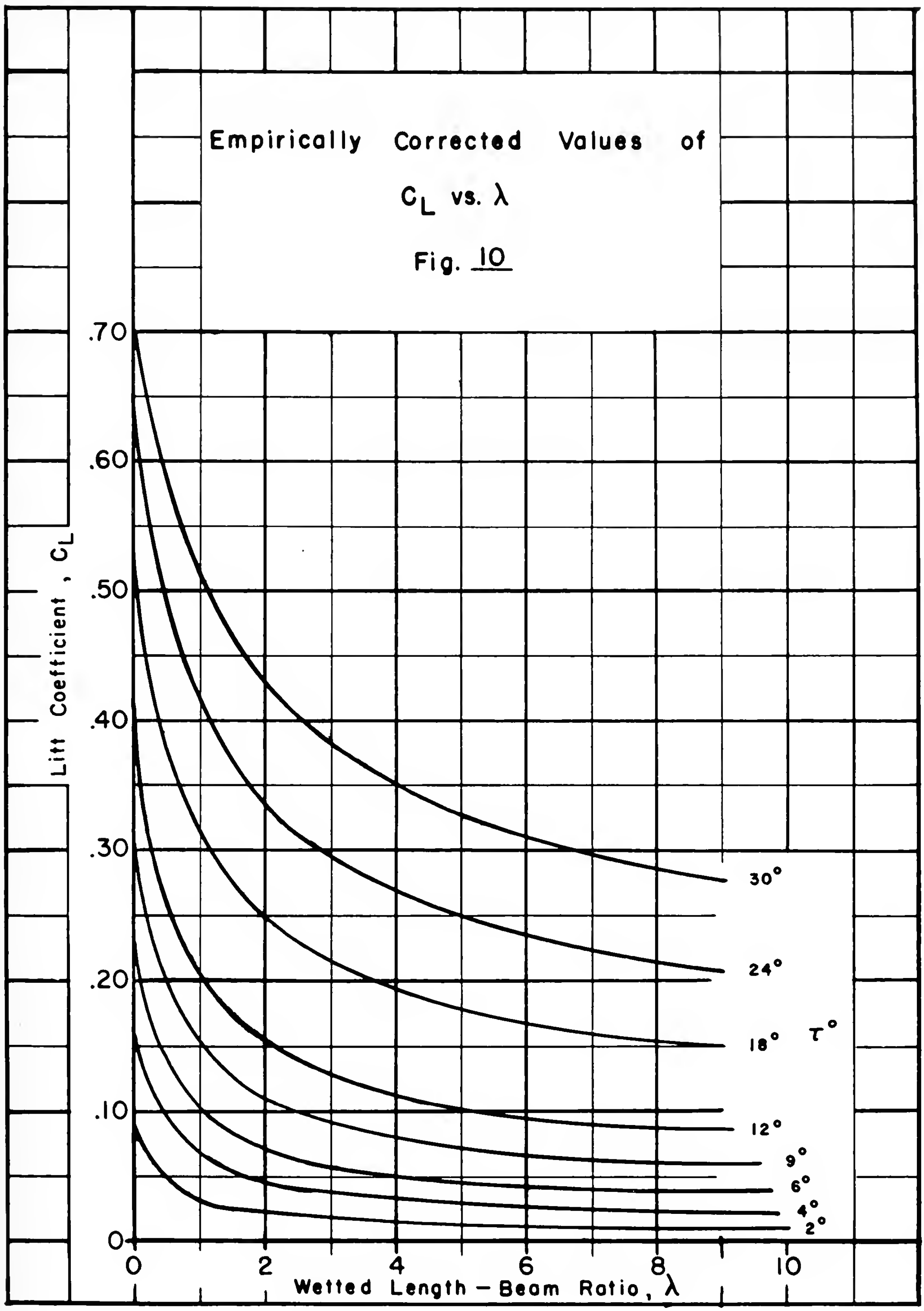

Empirically Corrected Values of
C_L vs. λ
Fig. 10
Lift Coefficient, C_L
.70
.60
.50
.40
.30
.20
.10
0
0
2
4
6
8
10
Wetted Length – Beam Ratio, λ
30°
24°
18°
τ°
12°
9°
6°
4°
2°

Comparison of the Computed Lift Coefficient
with Experimental Data

Fig. 11

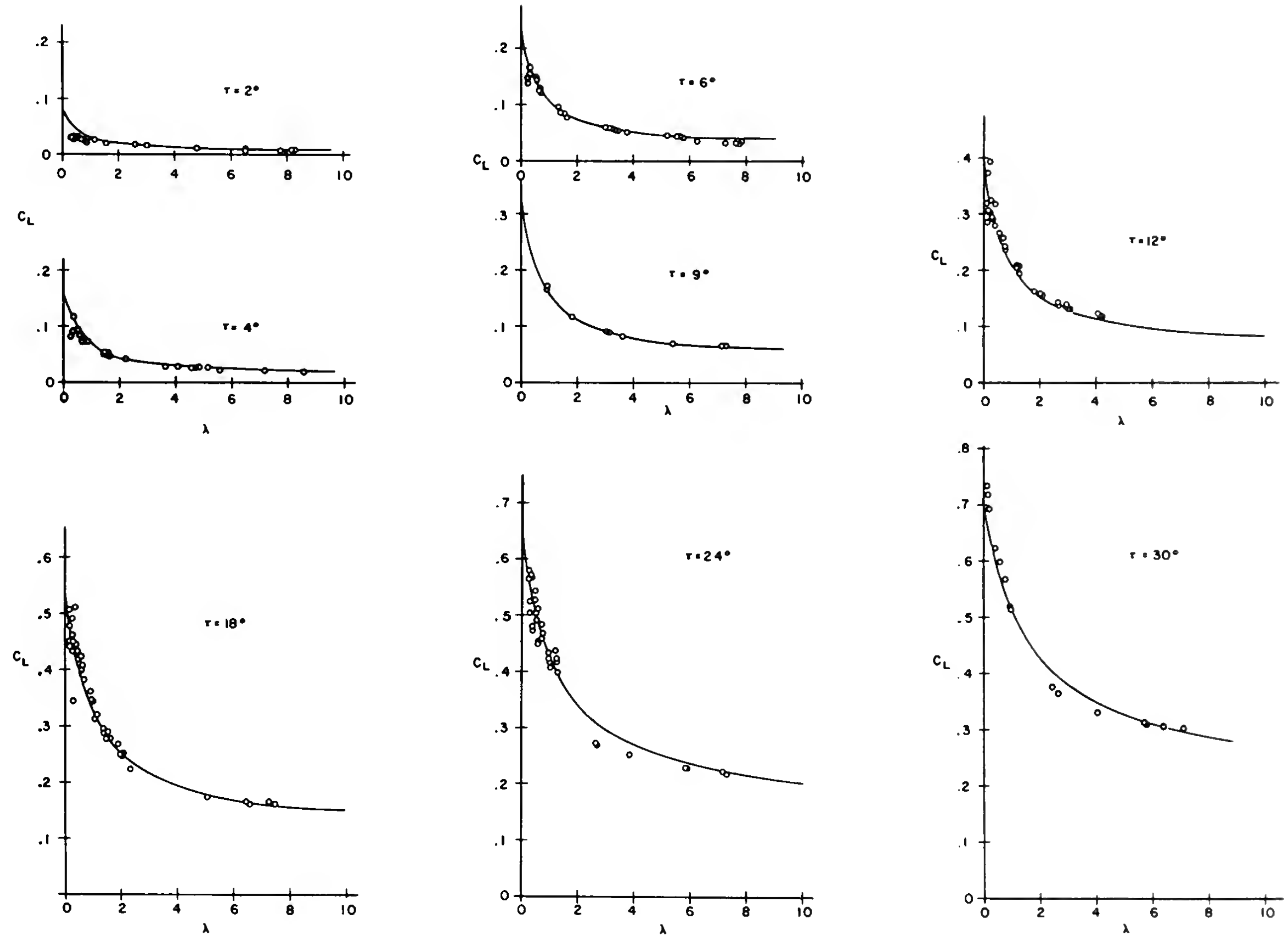

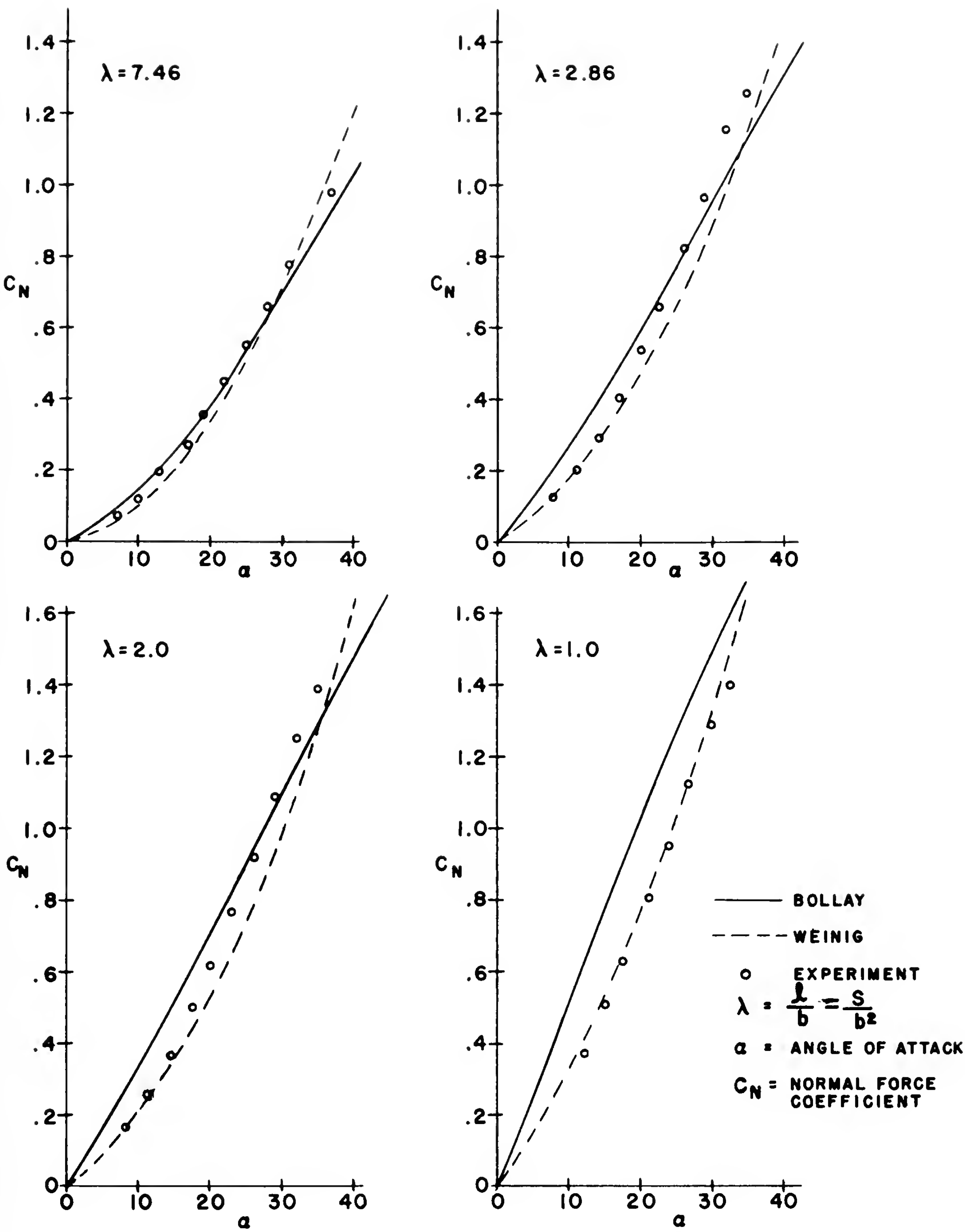

COMPARISON of WEINIG and BOLLAY AIRFOIL THEORIES
for the EFFECT of LOW ASPECT RATIO

Fig. 12

LIFT COEFFICIENT vs. ANGLE OF ATTACK
for FLAT PLATE AIRFOILS

Fig. 13

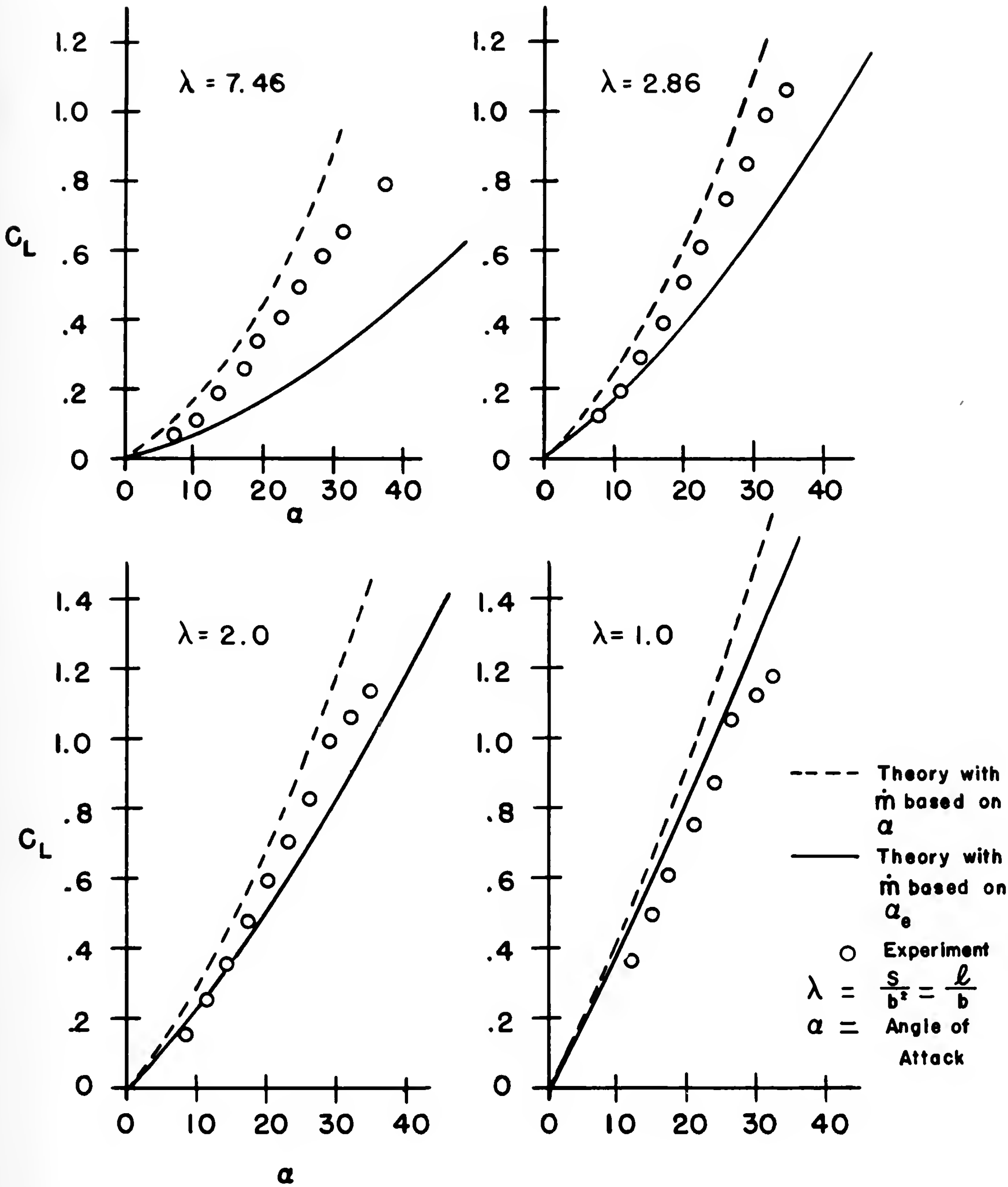

Figures for APPENDIX II

Fig. 14

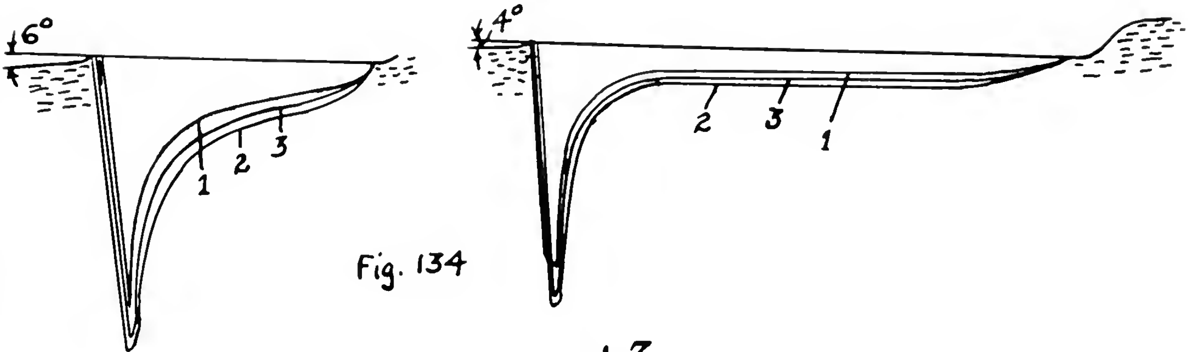

Fig. 134

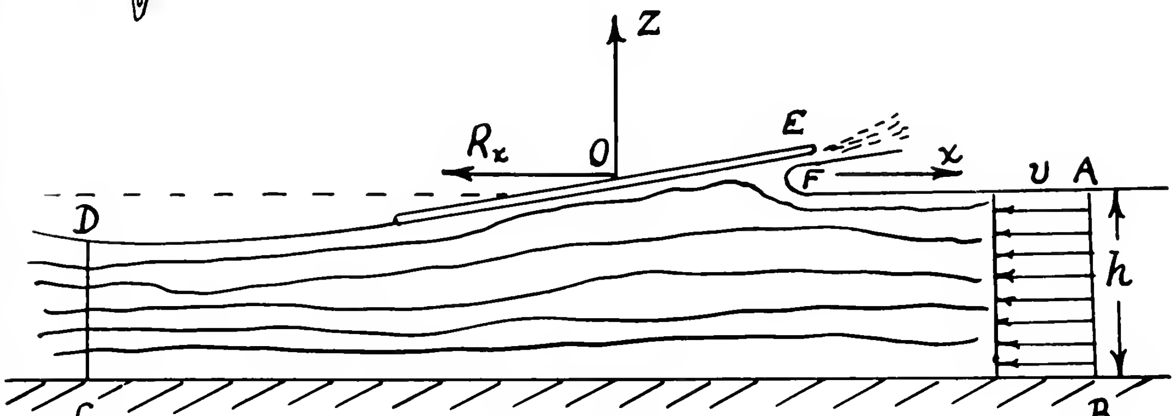

Fig. 135

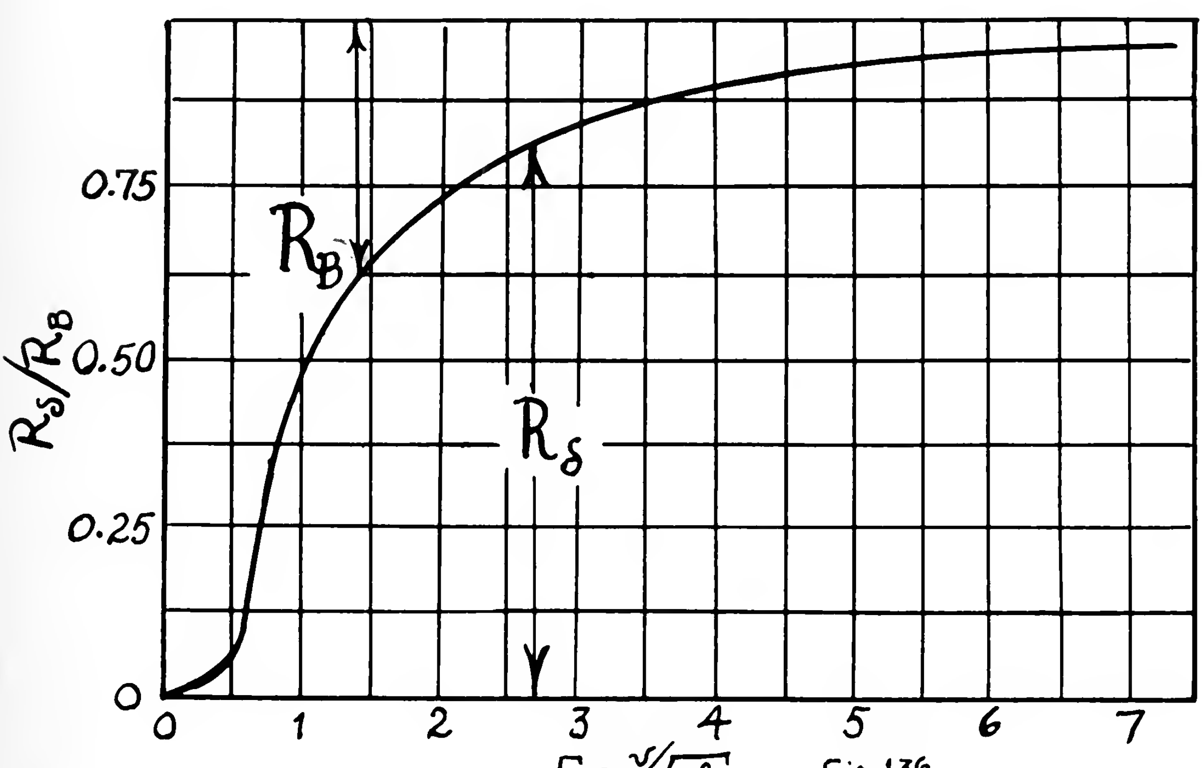

Fig. 136

Fig. 14 (cont'd)

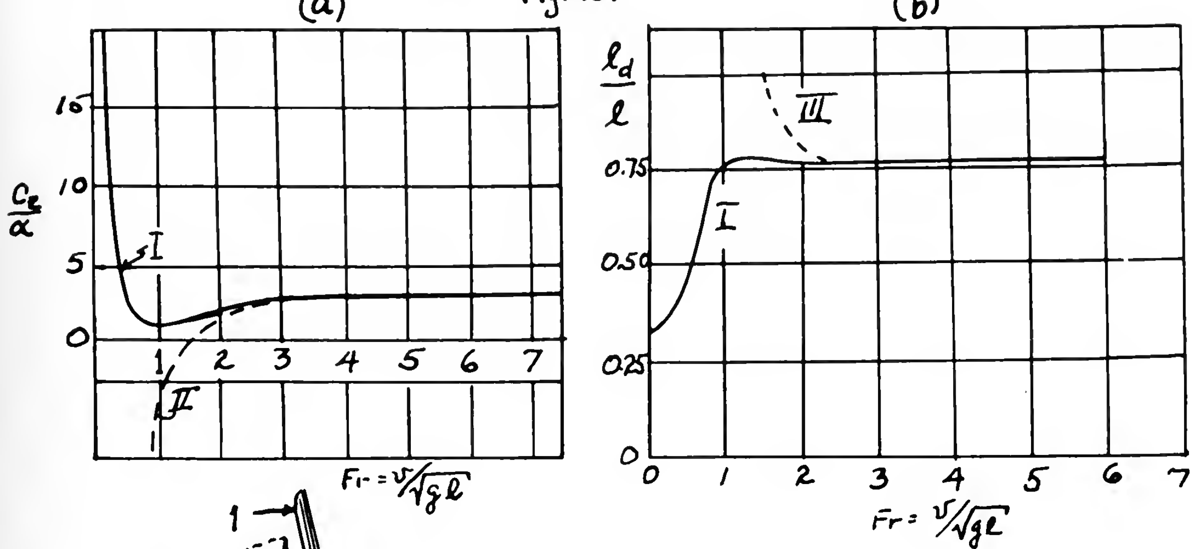

Fig. 137

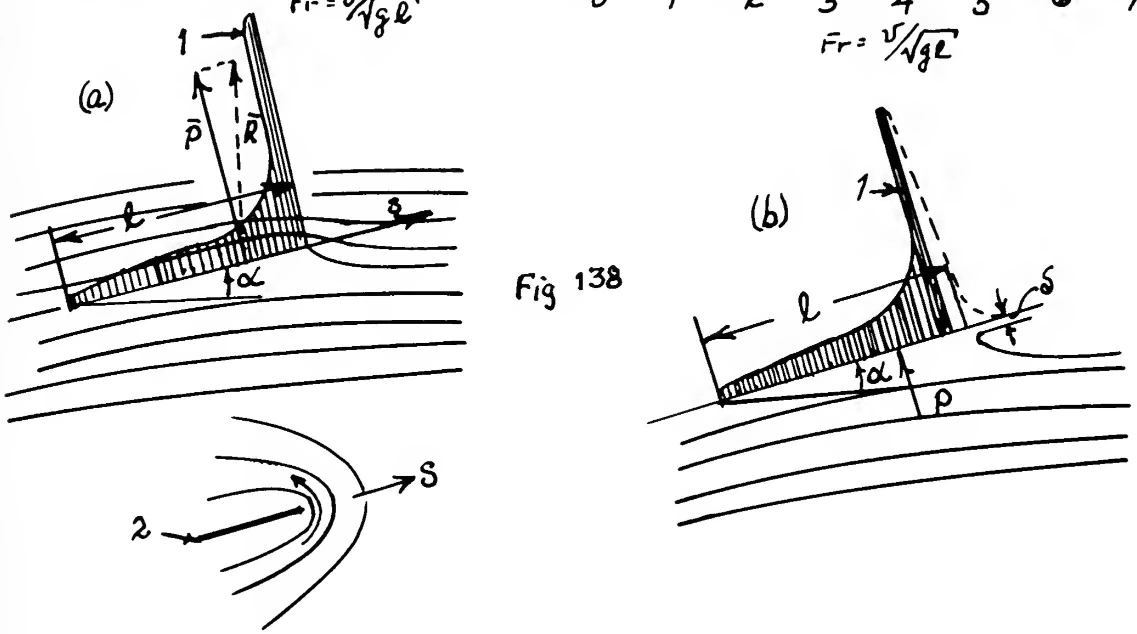

Fig 138

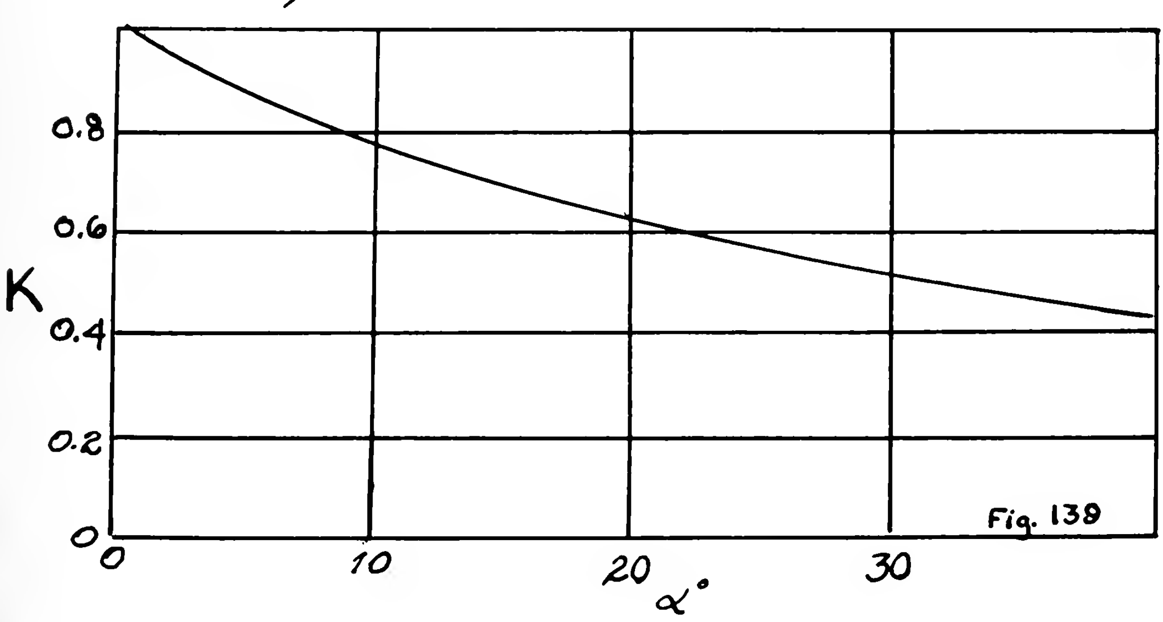

Fig. 139

Thesis
F236

28934

Farshing
The lift coefficient of flat
planing surfaces.